Marine Environmental Research 190 (2023) 106098

Contents lists available at ScienceDirect

Marine Environmental Research

journal homepage: www.elsevier.com/locate/marenvrev

Short-term response of macroalgal communities to ocean warming in the Southern Bay of Biscay

O. Arriaga [a,*], P. Wawrzynkowski [b,1], H. Ibáñez [a], N. Muguerza [a], I. Díez [a], I. Pérez-Ruzafa [c], J.M. Gorostiaga [a], E. Quintano [a], M.A. Becerro [b]

[a] Laboratory of Botany, Department of Plant Biology and Ecology, Fac. of Science and Technology & Research Centre for Experimental Marine Biology and Biotechnology PIE-UPV/EHU, University of the Basque Country (UPV/EHU), PO Box 644, 48080, Bilbao, Spain
[b] The BITES Lab, Center for Advanced Studies of Blanes (CEAB-CSIC), Access Cala S Francesc 14, 17300, Blanes, Girona, Spain
[c] Department of Biodiversity, Ecology and Evolution, Complutense University of Madrid (UCM), C/José Antonio Novais, 12, 28040, Madrid, Spain

ARTICLE INFO

Keywords:
Climate change
Temperature
Macroalgae
Community temperature index (CTI)
Canopy
Subtidal
Iberian Peninsula
Monitoring

ABSTRACT

Climate change is causing significant shifts in biological communities worldwide, including the degradation of marine communities. Previous research has predicted that southern Bay of Biscay canopy-forming subtidal macroalgal communities will shift into turf-forming Mediterranean-like communities by the end of the century. These predictions were based on a community-environment relationship model that used macroalgal abundance data and IPCC environmental projections. We have tested the short-term accuracy of that model by resampling the same communities and locations four years later and found the short-term predictions to be consistent with the observed communities. Changes in sea surface temperature were positively correlated with changes in the Community Temperature Index, suggesting that macroalgal communities had responded quickly to global warming. The changes over four years were significant, but canopy-forming macroalgae were more resilient in local sites with favourable temperature conditions. Our study demonstrated that updating predictive models with new data has the potential to yield reliable predictions and inform effective conservation strategies.

1. Introduction

Anthropogenic activities, especially the combustion of fossil fuels, have led to a concerning increase in greenhouse gas emissions and a significant warming of the Earth (Al-Ghussain, 2019). Since 1880, Earth's temperature has risen by 0.08 °C per decade, but that figure has more than doubled since 1981 to a current rate of 0.18 °C per decade (Lindsey and Dahlman, 2022). The average temperature of the planet's land and ocean surface in 2021 was 1.06 °C warmer than in pre-industrial times (1880–1900; NOAA, 2023). The ocean has absorbed more than 90% of the excess heat, which has led to an increase in the Ocean Heat Content (OHC) in the upper 2000 m layer of the world's oceans (Cheng et al., 2021). Due to the expected increase in OHC, Earth will likely reach 1.5 °C above pre-industrial levels in the near term (2021–2040) unless we take significant measures to reduce carbon emissions (IPCC, 2023).

Temperature plays a crucial role in shaping species distributions (Chen et al., 2011; Tittensor et al., 2010). Global warming is causing many species worldwide to shift poleward, both on land (Chen et al., 2011; Devictor et al., 2012) and in the oceans (Kortsch et al., 2015; Kumagai et al., 2018; Pinsky et al., 2020). Marine species are shifting poleward at an average rate of 72 km per decade, a full order of magnitude faster than the rate for terrestrial species (Poloczanska et al., 2013). This shift means that the "warming" or "thermophilisation" of biological communities is one of the main consequences of global change (Bowler and Böhning-Gaese, 2017; Parmesan and Yohe, 2003). In many temperate areas, cold-adapted species are declining while warm-adapted species are increasing in relative abundance (Gottfried et al., 2012).

Macroalgae are important primary producers and ecosystem engineers that modify their environment and offer shelter and food for associated organisms (Harley et al., 2012). They also provide many

* Corresponding author.
E-mail addresses: olatz.arriaga@ehu.eus (O. Arriaga), hibanez003@ikasle.ehu.eus (H. Ibáñez), nahiara.muguerza@ehu.eus (N. Muguerza), isabel.diez@ehu.eus (I. Díez), iperuz@ucm.es (I. Pérez-Ruzafa), jm.gorostiaga@ehu.eus (J.M. Gorostiaga), endika.quintano@ehu.eus (E. Quintano), mikel.becerro@csic.es (M.A. Becerro).
[1] University of Girona, Institute of Aquatic Ecology, C/Maria Aurèlia Capmany 69, Girona, E-17003, Catalonia, Spain. paul.wawrzynkowski@udg.edu

https://doi.org/10.1016/j.marenvres.2023.106098
Received 8 March 2023; Received in revised form 4 July 2023; Accepted 7 July 2023
Available online 8 July 2023

ecosystem goods and services since they operate as carbon sinks and help prevent environmental disturbances such as storms or floodings (Rönnbäck et al., 2007). There is ample evidence of macroalgal community degradation including a decrease in canopy-forming species that results in turf-dominated communities (Filbee-Dexter and Wernberg, 2018; Orlando-Bonaca et al., 2021), increased overgrazing leading to barren ground formation (Kumagai et al., 2018; Vergés et al., 2014), and the contraction and expansion of cold-affinity and warm-affinity species (Burrows et al., 2019; Smale and Wernberg, 2013; Wernberg et al., 2016). Macroalgal community degradation is a complex process driven by numerous intertwined factors. Temperature is often reported as the main driver of change and is the focus of our study. Yet, heat waves, storms, wave exposure, overgrowth by epiphytes, pollution, eutrophication, species invasion, or harvesting may also play a role and covary with warming (Borja et al., 2013, 2018; Fernández, 2011; Filbee-Dexter and Wernberg, 2018; Muguerza et al., 2017).

The Southern Bay of Biscay offers an excellent opportunity to investigate changes in macroalgal community structure resulting from rising temperatures. First, the region has a strong thermal gradient, with a colder western part influenced by upwelling conditions during the summer and a warmer eastern part (Lavín et al., 2006). Second, the Cantabrian Sea that borders the northern coast of the Iberian Peninsula has warmed by 0.22 °C per decade since the 1970s (Chust et al., 2022; deCastro et al., 2009), exceeding the global trend of 0.15 °C per decade (Rhein et al., 2013). This warming trend is most prominent during spring and summer (Díez et al., 2012; Gómez-Gesteira et al., 2008, 2011; Izquierdo et al., 2022). Third, several studies report a marked decrease in canopy-forming subtidal macroalgae such as kelp species, the warm-temperate red algae *Gelidium corneum*, and the fucoid *Gongolaria baccata,* which have started to retract from the eastern end of the Cantabrian Sea towards the west (Borja et al., 2013; Casado-Amezúa et al., 2019; Díez et al., 2012; Fernández, 2011; Muguerza et al., 2017). At the westernmost region of the study area (Coast of Galicia), these changes are buffered by the effect of cold water upwellings in summer (Casado-Amezúa et al., 2019). However, less pronounced declines for several cold-temperate canopy-forming species have been recently reported off the Galician and northern Portuguese Coasts (Monteiro et al., 2022)."

A practical approach to shed light on the effect of temperature on macroalgal communities is to use thermal metrics that can target temperature effects alone. The Community Temperature Index (CTI) is the abundance-weighted mean of the species' optimal temperature. CTI helps understand the thermal preferences of birds (Bowler and Böhning-Gaese, 2017; Devictor et al., 2012), fish (Bowler and Böhning-Gaese, 2017; Burrows et al., 2019; Day et al., 2018), and invertebrates (Flanagan et al., 2019; Stuart-Smith et al., 2015). What little information is available on the thermal preferences of macroalgal communities stems primarily from experimental approaches for a few ecologically-relevant macroalgal species, but there is less information available at the community level of organisation (Anderson, 2006; Graba-Landry et al., 2020; Orfanidis, 1991).

Understanding how macroalgal communities will respond to global warming in the future is crucial for the study of the impact of climate change on benthic communities and for making predictions about future scenarios. Muguerza et al. (2022a) developed a community-environment relationship model for the northern Iberian Peninsula to forecast changes in subtidal macroalgal communities under multiple climate change scenarios. They found that water temperature is the primary factor influencing the distribution of macroalgal communities, while nutrient availability plays a secondary role. They suggested that northern Iberian communities could undergo a meridionalisation trend by the end of the century. This meridionalisation will occur from east to west (Muguerza et al., 2022a). However, to test the model's predictive capacity it is essential to gather updated biological and environmental data to see whether macroalgal communities are shifting and if so whether they follow the trend predicted by their model.

Here, we combined global species occurrence data with gridded temperature datasets to calculate the Species Temperature Index (STI) of over 200 macroalgal species and quantified the impact of temperature increase on macroalgal communities. After four years, we resampled the locations investigated in 2015 by Muguerza et al. (2022a) in their study. First, we quantified the actual short-term community shifts and determined their evolution. Second, we tested the model's short-term predictive capacity. To do so, we compared the model's predicted communities with the observed natural communities in 2019. Third, to isolate the role of temperature in the observed macroalgal shifts, we used species' thermal traits to calculate a Community Temperature Index (CTI). Even in the short term, we anticipated that some signs of the east-west meridionalisation forecasted by their model may become visible (H_0: no short-term community change). We expected a good correlation between modelled and observed communities (H_0: no predictive capacity of the model). Considering that Muguerza et al. (2022a) identified water temperature as the primary factor influencing the distribution of the species, and in the face of the ongoing global warming, we also hypothesized that SST could partially explain the observed community shifts (H_0: no correlation between changes in SST and changes in CTI).

2. Methods

2.1. Study area

In the summers of 2019–2020 (from July to September), we quantified species composition and abundance in the exact same locations sampled in 2015 by Muguerza et al. (2022a). We studied eight locations in the southern Bay of Biscay in 2019 (L1: Malpica; L2: Cedeira; L3: Luarca; L4: Lastres; L5: San Vicente; L6: Somocuevas; L7: Kobaron; and L8: Ea), and two reference locations in the Mediterranean Sea in 2020: one in the Alboran Sea (L9: La Herradura) and the other in the Western Mediterranean Sea (L10: Cabo Palos) (Fig. 1, Appendix a).

Our study area has notable differences in environmental conditions. We focus here on sea surface temperature (SST) and nitrate concentration (NIT) as the primary drivers of community change (Muguerza et al., 2022a). The southern Bay of Biscay has a distinct west-to-east thermal gradient, with a summer upwelling system that cools SST to 16 °C during upwelling conditions in the western area (Gómez-Gesteira et al., 2008). Here, SST ranges from 14 °C in winter to 19.5 °C during summer downwelling conditions (Gómez-Gesteira et al., 2008; Ospina-Alvarez et al., 2010). The influence of this upwelling weakens towards the east, mainly because Cape Peñas acts as a boundary for the upwelling system's area of influence (Lavín et al., 2006; Valencia et al., 2004). Consequently, the range of annual variation in SST in the easternmost area is higher than in the western area, ranging from 12 °C in winter up to 22 °C in summer (Borja et al., 2000).

The locations on the Mediterranean Sea are warmer on average, with SST in the Alboran Sea ranging from 15.5 °C in winter to 22.8 °C in summer (Shaltout and Omstedt, 2014). Proximity to the Atlantic Ocean and the influence of an upwelling system that mainly occurs during spring and summer cool the Alboran Sea SST to 17 °C during these months. The Western Mediterranean Sea is warmer than the Alboran Sea, with SST ranging between 15 °C in winter and 25 °C in summer (Shaltout and Omstedt, 2014).

Nitrate concentration in surface waters is lower in summer due to the stratification of the water column, and higher in winter due to the mixing induced by waves and wind (Serret et al., 1999). In the western area of the Southern Bay of Biscay, nitrate concentration ranges from 0.3 mmol m^{-3} in summer to around 5 mmol m^{-3} in winter (González-Gil et al., 2018), whereas in the eastern area these values are around 1 mmol m^{-3} in summer to 4–5 mmol m^{-3} in winter (Baña et al., 2020; Muñiz et al., 2018). In the Alboran Sea, nitrate concentration ranges from $5 * 10^{-4}$ mmol m^{-3} in summer to $1.2 * 10^{-3}$ mmol m^{-3} in winter (Lazzari et al., 2016). However, the summer upwelling systems in the southwest Bay of Biscay and in northern Alboran Sea bring up deep,

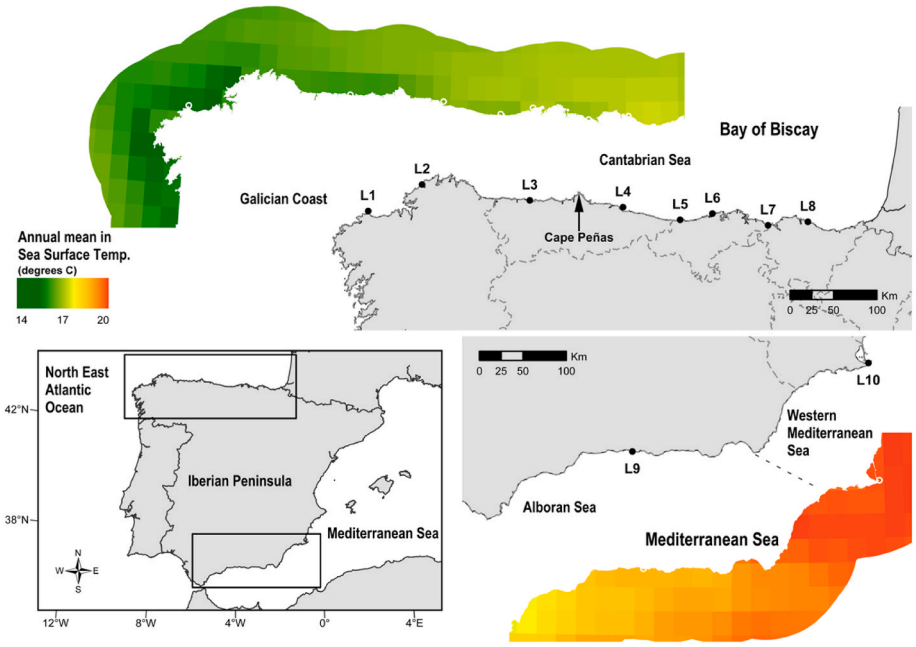

Fig. 1. Map of the study area showing the ten sampling locations (L1: Malpica; L2: Cedeira; L3: Luarca; L4: Lastres; L5: San Vicente; L6: Somocuevas; L7: Kobaron; L8: Ea; L9: La Herradura; and L10: Cabo Palos) and the mean sea surface temperature distribution for 2019, from Copernicus database. Source: own elaboration generated by ArcGIS Pro 2.2.0 software (https://www.esri.com/en-us/arcgis/products/arcgis-pro/overview)".

nutrient-rich, cool waters. In south-eastern Bay of Biscay, this system has little or no influence, as evidenced by the increase in temperature and the stratification of the water column, so the nutrient input comes mainly from rivers (Fernández-Salas et al., 2015). The Western Mediterranean Sea is oligotrophic, since the influence of the Atlantic decreases towards the east, and the main input is riverine but it has a low annual precipitation rate (Valdes-Abellan et al., 2017). Here the nitrate concentration ranges from 7.4 * 10^{-4} mmol m^{-3} in summer to 1.3 * 10^{-3} mmol m^{-3} in winter (Lazzari et al., 2016).

2.2. Data collection

2.2.1. Field data collection

Following the same methodology as Muguerza et al. (2022a), we conducted sampling at 5 m below chart datum. Two sites were selected per location, at least 15 m apart. We randomly placed eight 50 × 50 cm surfaces within each site at least 1 m apart, on rocky platforms or stable rocks, flattened or gently sloping, and with low sedimentation levels, always avoiding special habitats such as crevices or boulders. We accessed the locations by boat and used SCUBA to quantify each surface's macroalgae composition and abundance *in situ*. To estimate abundance, we used a 5% interval-scale cover range (from 5 to 100%). For macroalgal cover below 5% we used a 1% interval-scale (1, 2, 3, 4, 5%). For macroalgal cover below 1% we assigned a value of 0.5% to the taxa. All vertical strata of the community were sampled (crustose, basal, canopy, and epiphytic strata) and thus, the total cover of the vegetation could exceed 100%. We followed the taxonomic nomenclature used in AlgaeBase (Guiry and Guiry, 2023). We identified taxa at the species level *in situ* whenever possible. Samples for taxa that could not be determined *in situ* (turf species) were collected and transported to the laboratory for further identification. Samples were transported in moistened cotton bags and frozen within a few hours. We used binocular and optical microscopes for reliable taxonomical identification, carried out by the same researchers in both periods (2015 and 2019–2020).

2.2.2. Environmental data collection

The environmental data included in this study was downloaded from E.U. Copernicus Marine Service Information (Merchant et al., 2019). SST was obtained from the Multi Observation Global Ocean 3D Temperature Salinity Height Geostrophic Current and MLD dataset (https://doi.org/10.48670/moi-00052) and NIT was obtained from the Global Ocean Biogeochemistry hindcast dataset (https://doi.org/10.48670/moi-00019), both with a spatial resolution of 0.25 × 0.25° (about 27.75 × 27.75 km) and a monthly temporal resolution.

2.3. Data treatment and analyses

2.3.1. Macroalgal community structure

In this study, we used square-root transformed species cover data based on Bray-Curtis distance to analyse the similarity between pairs of averaged site-samples. Square-root transformation was applied to reduce the strong influence of dominant taxa in community analyses and allow for a broader number of species to play a part (Clarke and Warwick, 2001). We used the cluster classification technique to explore potential macroalgal community groups and represented the results in a dendrogram. To determine what species contributed most to the similarity within groups, a similarity percentage analysis (SIMPER) was conducted. We compared the classification obtained in 2015 with that obtained in 2019–2020. We also examined the species richness for each year and location and assessed for any significant differences between years and locations. These analyses were performed using PERMANOVA + for PRIMER software (Anderson et al., 2008).

2.3.2. Predictive capacity of the model

Using distance-based linear models, Muguerza et al. (2022a) showed that spring SST and, to a lesser degree, winter NIT were the main environmental variables responsible for the variation in the spatial pattern of macroalgae. Using these predictor variables, they run three regressions to calculate "modelled ecological distances" for each pair of locations. To assess the predictive capacity of their model, they also calculated the "observed ecological distances", which are the distance between the centroids of locations detected in the nMDS (based on the matrix of similarities between macroalgal communities). They then plotted the "observed ecological distances" with the "modelled ecological distances". Here, to assess the predictive capacity of their model in the short term, we compiled monthly SST (°C) and NIT (mmol*m^{-3})

data from the cell grid at each sampling location for the year 2019 for the southern Bay of Biscay and 2020 for the Mediterranean locations. We determined a mean spring SST by averaging the SSTs for April, May, and June and a mean winter value by averaging the NITs for January, February, and March. We then used the updated environmental data to run the same model as Muguerza et al. (2022a) and obtained "modelled ecological distances" between all pairs of locations for 2019–2020. We also constructed a nMDS (based on the matrix of similarities between macroalgal communities) with the community data gathered in 2019–2020 to quantify the "observed ecological distances" four (and five for Mediterranean locations) years after the initial sampling by Muguerza et al. (2022a), using PERMANOVA + for PRIMER software (Anderson et al., 2008). We then correlated the modelled and observed ecological distances for 2019–2020 to test the model's ability to predict short-term macroalgal community changes. The Pearson correlation coefficient provided a quantitative estimate of the model's accuracy. We turned the modelled ecological distances between locations into similarity values (by subtracting this distance from 100) to construct a nMDS based on the model and compare it with the nMDS performed with the observed data.

2.3.3. Temperature and CTI correlation

The similarity between sites within each location was high (over 80% on average), so we conducted the following analyses at the location level. The model developed by Muguerza et al. (2022a) identified temperature as the primary environmental variable influencing community structure. Given that warming in the area was mainly observed during spring and summer (Díez et al., 2012; Gómez-Gesteira et al., 2008, 2011; Izquierdo et al., 2022), we used Distance-based linear model analysis (DISTLM) to examine the impact of mean annual SST, spring SST (April, May, June), and summer SST (July, August, September) on the macroalgal community structure. We plotted distance-based redundancy analyses (dbRDA) to visualise the relationship and determined which temperature-related variables best explained the observed variation in macroalgal community structure, using PERMANOVA (Anderson et al., 2008). We then correlated this environmental variable with the Community Temperature Index (CTI).

For each recorded species, the Species Temperature Index (STI) was calculated as the average temperature of the species occurrence range, considered a proxy for the species' dependence on temperature (Devictor et al., 2012). We obtained the global distribution data for each species from the open-access databases "Ocean Biodiversity Information System" (OBIS) (https://www.obis.org/) and "Global Biodiversity Information Facility" (GBIF) (https://www.gbif.org/), by using the special packages robis (Provoost and Bosch, 2019) and rgbif (Chamberlain et al., 2021) from the open-source software R (R Development Core Team, 2023; RStudio Team, 2016). The time-frame considered for the distribution data was 1993–2020. We downloaded monthly SST data for the sites of occurrence of every species from the Copernicus database to calculate annual means. We calculated the CTI for each sampling unit to measure the average thermal affinity of the macroalgal communities. The CTI is the abundance-weighted STI average of all species in a sampling unit (Devictor et al., 2008, 2012). We then calculated the average CTI for each location and year. Differences in CTI were tested with a univariate PERMANOVA analysis based on Euclidean distance with time and location as fixed and random factors, respectively. For *post-hoc* pairwise comparisons Gosset t-statistic was used (Anderson et al., 2008).

Macroalgal species have varying lifespans and many have a life cycle that exceeds one year (i.e. *Gelidium corneum*), so current and past environmental conditions may determine the current state of the community (Chust et al., 2022; Ramos et al., 2020). To test the degree of association between temperature and CTI, we analysed the correlation between the change in temperature and the change in CTI. SST changes were calculated using the mean of the sampling year and the two previous years and compared 2017–2019 (2018–2020 for the Mediterranean) to 2013–2015 to accommodate the multiannual SST variance that multiple macroalgal species may experience (Appendix b). For the CTI change, we calculated the difference between CTI values in 2019 (2020 for Mediterranean locations) and 2015.

3. Results

3.1. Changes in the community structure

Based on the 43% similarity level used by Muguerza et al. (2022a), we found locations clustered in four groups with distinct species compositions. We found three geographic areas in the Southern Bay of Biscay macroalgal communities (western, central, and eastern sections) and another in the Mediterranean (Fig. 2b). The kelp *Saccorhiza polyschides* and the geniculate calcareous macroalga *Corallina officinalis* dominated in the westernmost Bay of Biscay locations (Group A: L1, L2, and L3). *Gelidium corneum* and the encrusting Corallinales *Mesophyllum expansum* dominated in the central Bay of Biscay locations (Group B: L4 and L6). *Mesophyllum expansum* and the ephemeral filamentous Ceramiales *Aphanocladia stichidiosa* dominated in the easternmost Bay of Biscay locations (Group C: L5, L7, and L8). The Corallinales *Lithophyllum incrustans* and *Jania pedunculata* var. *adhaerens* dominated the Mediterranean locations (Group D: L9 and L10). See Appendix c for a visual representation of these species in each location.

The three sections in the southern Bay of Biscay remained distinct in 2019 and 2015, although Group A was slightly more similar to Groups B and C in 2019 (33.15%) than in 2015 (29.75%). Location composition in the central section differed from 2015 to 2019 (Appendix d). L5 shifted from the central area in 2015 to the eastern area in 2019. In four years, the percent cover of *Gelidium corneum* in this location decreased from 59.1% to 23.4%, while the percent cover of *Aphanocladia stichidiosa* increased from 0% to 7.2% (Appendix e).

We also found the two Mediterranean macroalgal communities to be more similar in 2020 (54.13%) than in 2015 (38.63%). *Lithophyllum incrustans* and *Jania pedunculata* var. *adhaerens* replaced previously dominant species *Halopteris scoparia* and *Padina pavonica* in the Mediterranean locations (Appendix d). Undetected in 2015, *Jania pedunculata* var. *adhaerens* showed a percent cover of 15.63 in the Alboran Sea and 50.63 in the western Mediterranean in 2020 (Appendix e).

The species richness also differed from one location and year to another, except in Ea (L8) (Fig. 3, Appendix f). The lowest value corresponded to Somocuevas (L6) in both surveys (a mean of 12 taxa in 2015 and a mean of 8 taxa in 2019). The highest values were found in the two Mediterranean locations and in Luarca (L3) (around 27 taxa in 2015 and 34 in 2019), followed by north-eastern locations. In four years, the number of taxa decreased in the westernmost location (L1, from 19 to 14) and in the central group (L4, from 27 to 19 and L6 from 12 to 8), but in the other locations an average increase of 7 taxa was observed (Fig. 3).

3.2. Predictive capacity of the model

We found a positive correlation ($R = 0.740$, $p < 0.0001$) between the observed and modelled spatial distribution in 2019–2020 (Fig. 4).

Overall, locations from the southern Bay of Biscay (L1 to L8) were closer to each other than forecasted, particularly Cedeira (L2), i.e, they were more similar in species composition and abundance. Contrary to model's predictions, the locations here did not follow a succession along the coast, but instead, they became more similar, they homogenized. Somocuevas (L6) remained more distinct from the other northern locations, and San Vicente (L5) shifted closer to the eastern communities of Kobaron (L7) and Ea (L8) in the observed pattern. The Mediterranean locations of La Herradura (L9) and Cabo de Palos (L10) remained distant from the Bay of Biscay locations but were more similar than the model predicted (Fig. 5).

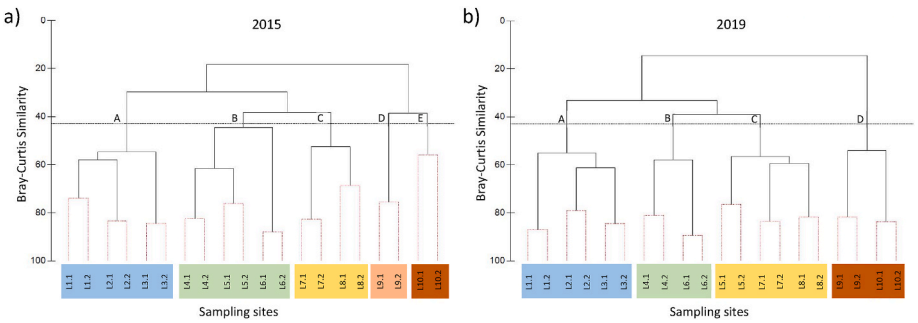

Fig. 2. Hierarchical clustering dendrogram of sampling sites, based on Bray-Curtis similarities calculated on square-root transformed abundance data. Dashed lines indicate the 43% similarity level. "L" refers to location (L1: Malpica; L2: Cedeira; L3: Luarca; L4: Lastres; L5: San Vicente; L6: Somocuevas; L7: Kobaron; L8: Ea; L9: La Herradura; and L10: Cabo Palos). Each location had two replicated sites, labelled as "0.1" and "0.2". a) 2015, b) 2019–2020.

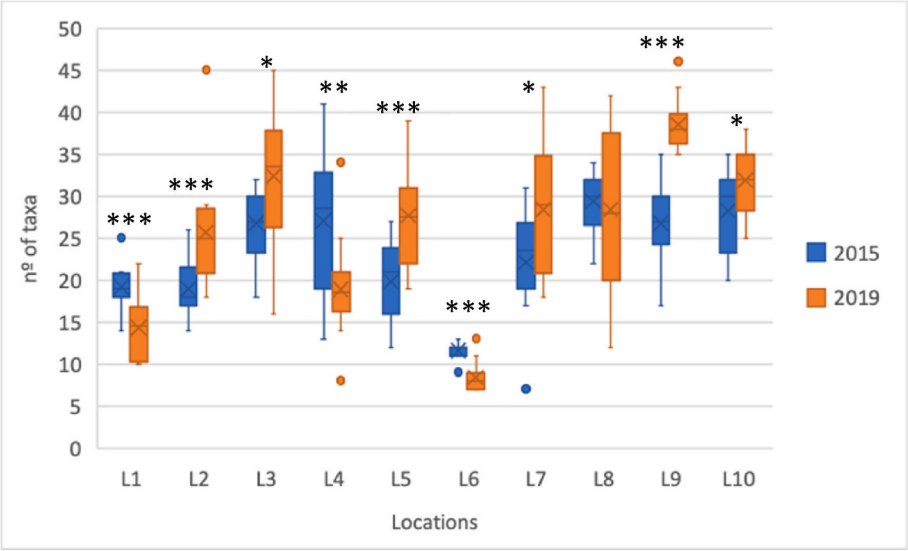

Fig. 3. Average number of taxa per surface for each location in 2015 and 2019–2020. "L" refers to location (L1: Malpica; L2: Cedeira; L3: Luarca; L4: Lastres; L5: San Vicente; L6: Somocuevas; L7: Kobaron; L8: Ea; L9: La Herradura; and L10: Cabo Palos). Asterisk indicate significant differences between years within each location: *p < 0.05, **p < 0.01, ***p < 0.001.

3.3. The effect of temperature on spatial distribution

Annual SST and summer SST (SSTsu) were the best fit-explanatory variables, explaining 42.4% of the total variation (Distance-Based Linear Model, distLM). Annual SST discriminated between the Southern Bay of Biscay and Mediterranean communities, and SSTsu discriminated within the Southern Bay of Biscay communities, following an east-west gradient (Fig. 6, Appendix g). Annual SST also distinguished between the two periods for the Mediterranean locations and for locations L4 to L8, whereas for locations L1 to L3 the difference between the two periods was established by summer SST.

We also found significant differences in the Community Temperature Index (CTI) across locations and years (Fig. 7, Appendix h). Mediterranean locations (L9 and L10) showed the highest CTI values both in 2015 and 2020, with average values ranging from 14.7 °C to 16.34 °C in L9, and 16.5 °C to 17.3 °C in L10. The westernmost locations of the Bay of Biscay had the lowest CTI values, with average values of 13.5 °C in 2015, and 13.3 °C in 2019 (Fig. 7). CTI also varied from year to year in six out of the ten locations (Fig. 7). On average, CTI decreased by 2.38% at L1, L2, L3 (Group A), and L8, but increased by 4.88% at the remaining locations. We found a significant positive correlation between the changes in SSTsu and in CTI ($R = 0.835$, $p = 0.003$, Fig. 8).

4. Discussion

Accurately predicting the impact of global change on marine benthic communities is crucial to help preserve our ecosystems and the services they provide. While models can help us simulate potential effects, inform preventive measures, and aid in adaptation strategies, validating their accuracy using real-world data is crucial. Muguerza et al. (2022a) used spatial data to forecast that macroalgal communities in the Cantabrian Sea would resemble those in the Mediterranean region more closely than those along the Galician coast by the end of the century, which would follow an east-to-west gradient. Our study focused on testing the short-term predictions of this model using new observational data gathered four years after the initial assessments. Despite relying on spatial data for long-term projections, we found that the short-term predictions aligned with actual observations of the same communities, indicating the model's robustness (Muguerza et al., 2022a). Short-term temperature changes were positively correlated with changes in the Community Temperature Index (CTI), suggesting that macroalgal communities quickly adapt to temperature changes, potentially triggering the observed phase shift in the region. We also detected discrepancies between the model's projections and the observed communities, providing additional insights into climate-induced changes in community composition.

In our study, locations west of Cape Peñas (L1, L2, and L3) formed a

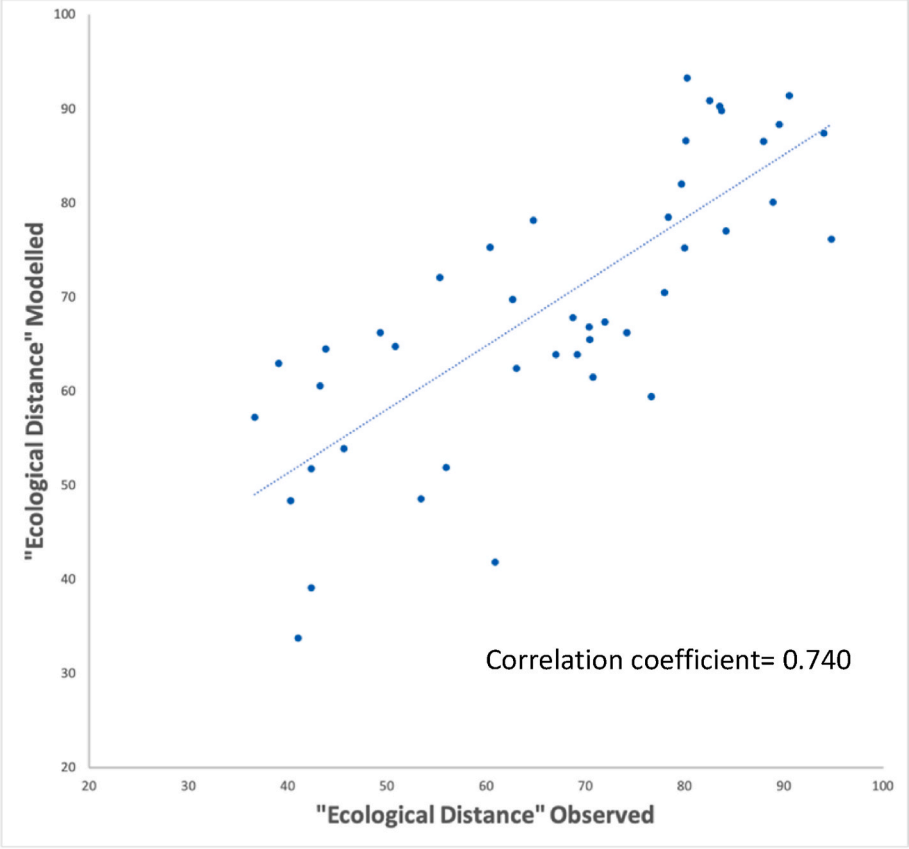

Fig. 4. Association (linear regression) between the observed and modelled ecological distances for 2019–2020. Ecological distance is the distance between centroids as detected in the non-metric multidimensional scaling (nMDS).

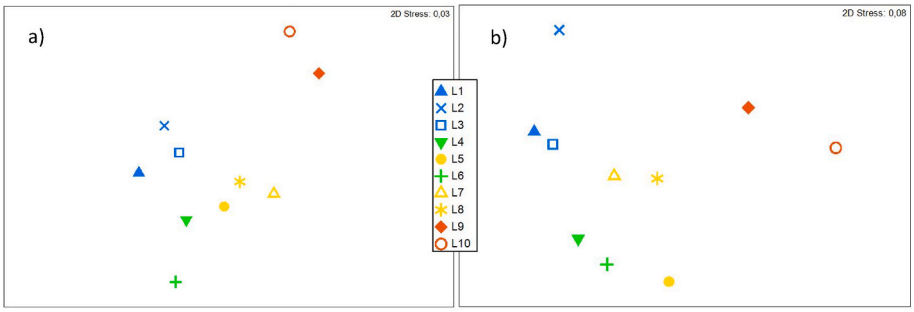

Fig. 5. Non-metric multidimensional scaling (nMDS) diagrams (Anderson et al., 2008) of the 10 locations (L1: Malpica; L2: Cedeira; L3: Luarca; L4: Lastres; L5: San Vicente; L6: Somocuevas; L7: Kobaron; L8: Ea; L9: La Herradura; and L10: Cabo Palos) based on square-root transformed abundances and Bray-Curtis similarities. a) observed pattern. B) modelled pattern. Colours are based on 43% similarity clustering (Fig. 2b).

consistent geographic section characterized by the warm-temperate kelp *Saccorhiza polyschides*, with a thermal optimum of 10.3 °C (Casado-Amezúa et al., 2019; Fernández, 2016; Muguerza et al., 2017). East of Cape Peñas, a central region (L4, L6) was dominated by the canopy-forming *Gelidium corneum*, which has a thermal optimum of 12.5 °C, and the easternmost area (L5, L7, and L8) was dominated by the morphologically simple *Aphanocladia stichidiosa*, with a thermal optimum of 17.2 °C (Casado-Amezúa et al., 2019; Muguerza et al., 2022a). These distribution patterns align with previous studies describing the retreat of *S. polyschides* and *G. corneum* toward the west (Assis et al., 2017; Borja et al., 2018; Gorostiaga 1995). Muguerza et al. (2022a) already reported this same distribution of the dominant species in 2015, showing a thallus size decrease with increasing temperature, which leads to a structural simplification of the communities.

Our analyses revealed changes in the distribution of dominant canopy-forming species from 2015 to 2019, supporting the predicted east-west meridionalisation of the southern Bay of Biscay (Muguerza et al., 2022a). Specifically, the macroalgal communities of San Vicente (L5) shifted from the central section to join the eastern area, accompanied by a decrease in the cover of *G. corneum* and an increase in the number of taxa (Díez et al., 2012; Muguerza et al., 2017). This transition resulted in a community dominated by morphologically simple forms (*Aphanocladia stichidiosa* and *Ceramium* spp.) and coralline species (*Jania squamata*, *Ellisolandia elongata*, and *Corallina officinalis*), which is consistent with the phase shifts from canopy-dominated macroalgal communities to turf-forming communities observed worldwide (Benedetti-Cecchi et al., 2001; Díez et al., 2012; Perkol-Finkel and Airoldi, 2010; Smale and Wernberg, 2013; Voerman et al., 2013; Wernberg et al., 2016). Notably, we also found that the Mediterranean communities have undergone more significant changes and have become more

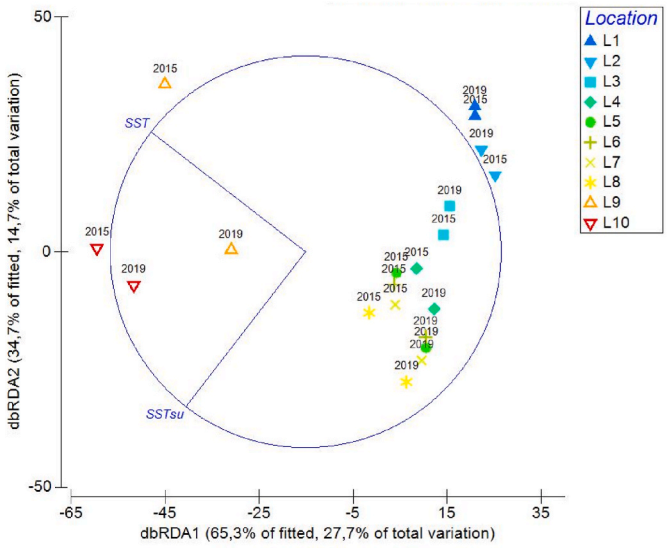

Fig. 6. Distance-based redundancy analysis (dbRDA) ordination plots showing the relationship between the temperature-related environmental variables that best explain the variation of macroalgal communities for 2015 and 2019–2020. L1: Malpica; L2: Cedeira; L3: Luarca; L4: Lastres; L5: San Vicente; L6: Somocuevas; L7: Kobaron; L8: Ea; L9: La Herradura; and L10: Cabo Palos. SST (annual sea surface temperature). SSTsu (summer sea surface temperature). The colour gradient represents the SSTsu gradient along the study area.

homogeneous, with a shift towards coralline-dominated communities. Increased temperature, water transparency, and solar radiation may have stimulated coralline calcification and growth rates (Díez et al., 2012; Jian-Zhang et al., 2010; Steller et al., 2007). However, it is uncertain whether these findings apply to the broader Mediterranean region, as our study primarily focused on the southern Bay of Biscay and included only two Mediterranean locations as references (Muguerza et al., 2022a; Ramos et al., 2020).

Discrepancies between the model projections and the observed communities also provided insights into the complex dynamics of climate-driven community changes. For example, the model predicted reduced distances between Somocuevas (L6) and the eastern locations, but actual observational data did not support these predictions. The unique characteristics of Somocuevas (L6), situated near the mouth of the River Pas and influenced by its freshwater input, may explain the disparity between the model and reality. The river's current freshwater inflow likely cools the water and provides additional nutrients, supporting the thriving *Gelidium corneum* communities in this area (Gorostiaga, 1995). Somocuevas (L6) exhibited the best-preserved *G. corneum*-dominated community in our study, characterized by low species richness and floristic homogeneity, consistent with other *G. corneum*-dominated communities such as Lastres (L4, see Appendix d).

Our study revealed an increase in *G. corneum* and associated epiphytic species (*Dictyota dichotoma* and *Plocamium cartilagineum*) in Lastres (L4). Conversely, we observed a decrease in coralline (*Ellisolandia elongata*, *Corallina officinalis*, and *Jania rubens*) and Ceramiales (*Gayliella flaccida*, *Microcladia glandulosa*, *Vertebrata fruticulosa*) species (see Appendix d). The *G. corneum* canopy expansion led to a significant decrease in species richness. In the summer of 2014, before our initial sampling, Lastres (L4) experienced the highest summer temperature of the entire decade (2010–2020), causing an imbalance in the *G. corneum* community, manifested by stress symptoms such as frond yellowing and an increase in epiphytic ceramiaceous species. Similar stress symptoms occurred in San Vicente (L5) during the same year. However, unlike San Vicente (L5), which continued to deteriorate progressively in 2019, macroalgal communities in Lastres (L4) displayed greater resilience, with an increased percent cover of *G. corneum*. The cooler water temperature and potentially more nutrient-rich conditions in Lastres (L4) compared to San Vicente (L5) may account for the success of *G. corneum* in Lastres, as observed in Somocuevas (L6), where *G. corneum* stands have thrived over time. This phenomenon may be analogous to the effects of upwellings in other coastal areas (Lourenço et al., 2016). The presence of refuge locations with favourable local environmental conditions, such as Somocuevas (L6), is ecologically and biologically significant as they can safeguard the genetic heritage of threatened foundational species in the face of climate change effects (Assis et al., 2017; García et al., 2021). These findings underscore the importance of combining model predictions with empirical data to understand ecosystem responses to global change comprehensively.

Models are crucial to understand community shifts under global change, offering valuable insights into future scenarios and identifying

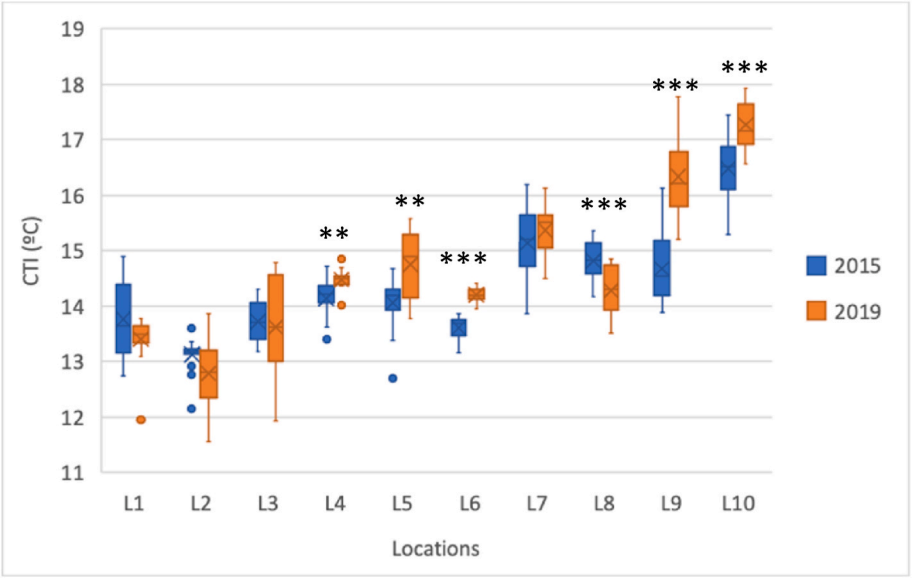

Fig. 7. Community Temperature Index (CTI) for each location in 2015 and 2019–2020. L1: Malpica; L2: Cedeira; L3: Luarca; L4: Lastres; L5: San Vicente; L6: Somocuevas; L7: Kobaron; L8: Ea; L9: La Herradura; and L10: Cabo Palos. Asterisk indicates significant differences from one year to another within each location: *p < 0.05, **p < 0.01, ***p < 0.001.

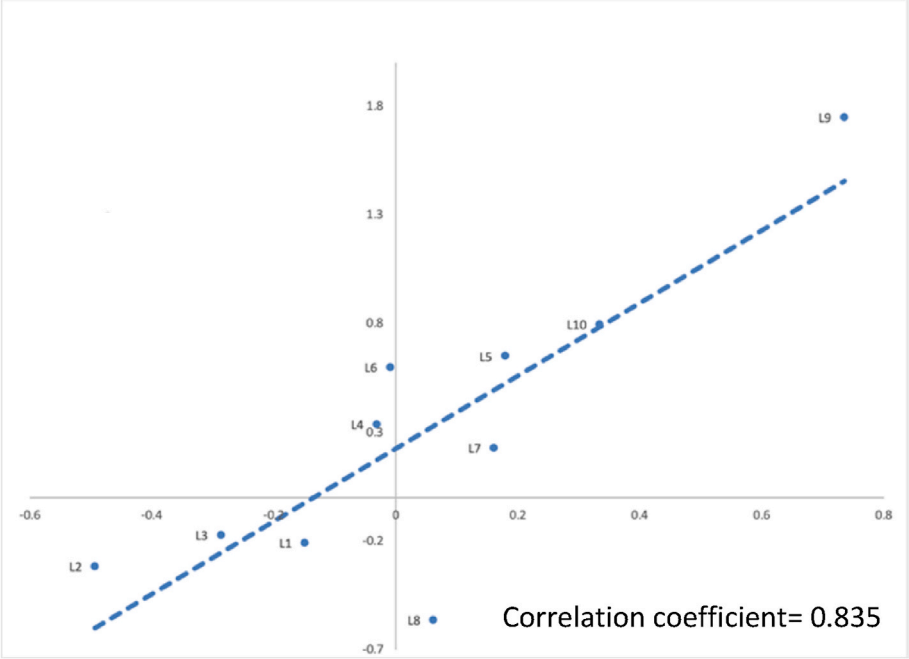

Fig. 8. Association (linear regression) between changes in summer SST (x axis) and changes in CTI (y axis). L1: Malpica; L2: Cedeira; L3: Luarca; L4: Lastres; L5: San Vicente; L6: Somocuevas; L7: Kobaron; L8: Ea; L9: La Herradura; and L10: Cabo Palos.

key drivers of ecological transformations. Here, we validated Muguerza et al.'s (2022a) model using real-world data and showed evidence of the model's consistency and accuracy in the short term, reinforcing the model's robustness. Yet, the model under discussion has some limitations. Firstly, there is a critical oversight in the model as it fails to consider biotic interactions, such as herbivory or competition for resources, which can strongly impact the organization and functioning of marine ecosystems (Falkenberg et al., 2013; Steneck et al., 2002). Secondly, collecting on-site environmental data, including temperature and nitrate concentration, would help obtain more precise estimates of local conditions. The model's current resolution (0.25° × 0.25°) covers over 750 km^2, which may not fully represent the local conditions of our sampling sites. Recording on-site environmental data could improve estimates of local conditions and the model's accuracy. The model would also benefit from accounting for the impact of riverine inputs or small upwelling systems, as these factors can significantly influence ecosystem dynamics. Finally, improving the model's accuracy could also involve increased replication and a broader spatial scale, including the western Iberian Peninsula and additional Mediterranean sites. However, given our goal of comparing Muguerza et al. (2022a) predictions to actual communities four years later, we could not modify the model.

There is increasing evidence worldwide that canopy-dominated macroalgal communities are shifting to structurally simpler alternate states (Benedetti-Cecchi et al., 2001; Fernández, 2016; Orlando-Bonaca et al., 2021; Perkol-Finkel and Airoldi, 2010; Wernberg et al., 2016). The factors behind phase shifts are numerous and intertwined, but temperature is an important parameter affecting species distribution (Husa et al., 2008; Müller et al., 2009; Sjøtun et al., 2015; Tittensor et al., 2010; Wernberg et al., 2016). Our data provided evidence to support the contention that the southern Bay of Biscay phase shift from three-dimensional macroalgal communities to turf-dominated communities may be temperature driven. Our study found a strong positive correlation between changes in water temperature and changes in the Community Temperature Index (CTI), suggesting that macroalgal communities responded quickly to ocean temperature change. The increasing temperature may favour species with warmer affinities and add stress to those with colder affinities, which may strongly influence species abundance and distribution. We used the Species Temperature Index (STI) as a proxy for thermal affinity. Given that the CTI is the abundance-weighted average of the STI, shifts in CTI represent changes in the thermal affinity of the system. A higher CTI represented a greater dominance of warmer species in the community, driven either by an increase in their percent cover or a decrease in the percent cover of colder affinity species (McLean et al., 2021). The southern Bay of Biscay has been warming since the early 80s (Anadón et al., 2009; Chust et al., 2022; Costoya et al., 2015; Fernández, 2011; Voerman et al., 2013). Colder affinity species, such *as Gelidium corneum* may be subjected to more significant stress, unlike warmer affinity species, such as ceramiaceous or coralline species, which may trigger the phase shift. We found one noteworthy exception to this pattern in Ea (L8), in the easternmost area of the southern Bay of Biscay. Contrary to expectations, the warm affinity species *Aphanocladia stichidiosa* and *Mesophyllum expansum* declined in this location. The reason behind this decline is unclear, given the rising temperatures and abundance trends of these species in the area over the last few decades (Muguerza et al., 2017, 2022b). This location had a bloom of *Ostreopsis siamensis* covering an estimated 25% of the substratum (author's observation). This epiphytic dinoflagellate is on the increase in the south-eastern Bay of Biscay (Drouet et al., 2021), and it contains several toxic chemicals that cause mortality in marine organisms, including macroalgae (Accoroni et al., 2015). The canopy that dominated the area was almost non-existent, and the community had shifted to small, fast-growing, opportunistic turf species.

Utilizing species' thermal traits to predict species distribution and abundance provides valuable insights into the impacts of climate change on marine communities. Our study showed that the Species Temperature Index (STI) and Community Temperature Index (CTI), in combination with SST predictions, enhance our understanding of how temperature influences community changes. The STI offers a proxy to evaluate species' responses to temperature variations by assessing thermal affinity. The CTI, as an abundance-weighted average of the STI, enables us to quantify changes in the thermal affinity of the entire community. Integrating these indices with SST projections would allow for more accurate predictions of future marine community shifts associated with climate change, empowering effective conservation and management strategies.

Global open-access databases are not perfect. The lack of abundance

data makes it difficult to accurately calculate species' thermal optimum. However, Webb et al. (2020) already showed a strong correlation between experimentally derived thermal maxima and the thermal affinity derived from matching global sea temperature databases with occurrence records. Our study provided further support for the usefulness of global datasets in calculating species' thermal traits. Given the speed and scale at which communities are shifting, the use of global open-access databases should not be overlooked in this context of rapid climate change. The information in those global databases may help us assess the vulnerability of thousands of species to global warming, find possible refugees for cold-affinity species, or protect those species at greater risk. In our study area, we found a location in the central area of the southern Bay of Biscay that operated as a refuge for cold-affinity species that were disappearing at adjacent sites. This is particularly significant since many studies provide evidence for a weakening intensity of the south-western Bay of Biscay upwelling system associated with changes in wind regimes (Gómez-Gesteira et al., 2011; Lemos and Pires, 2004; Pérez et al., 2010). The loss of the influence of upwelling in the southern Bay of Biscay could limit the distribution of kelp species to locally colder and nutrient-richer habitats.

In summary, accurate prediction of global change impacts on marine benthic communities is crucial for ecosystem preservation. Our study demonstrated that short-term predictions based on Muguerza et al.'s (2022a) model aligned with real-world observations, building confidence in predictive models. We observed deviations from the model, shedding light on climate-driven community changes. Temperature emerged as the primary driver, with macroalgal communities showing rapid responses. Given the widespread degradation of macroalgal communities worldwide, climate-driven macroalgal phase shifts may be a current reality rather than a long-term prediction. Testing ecological models may be crucial for predicting the impacts of global change on our natural communities.

Credit author statement

Olatz Arriaga: Conceptualization, Investigation, Methodology, Writing-Original Draft, Visualization. **Paul Wawrzynkowski**: Software, Data Curation, Formal analysis. **Hector Ibañez**: Investigation, Resources. **Nahiara Muguerza**: Investigation, Writing - Review & Editing. **Isabel Díez**: Investigation, Writing - Review & Editing. **Isabel Perez-Ruzafa**: Investigation, Resources. **Jose María Gorostiaga**: Conceptualization, Investigation, Writing - Review & Editing, Supervision, Funding Acquisition, Project administration. **Endika Quintano**: Investigation, Writing - Review & Editing, Supervision. **Mikel Becerro**: Conceptualization, Methodology, Writing - Review & Editing, Supervision, Funding Acquisition.

Declaration of competing interest

The authors declare that they have no known competing financial interests or personal relationships that could have appeared to influence the work reported in this paper.

Data availability

Data will be made available on request.

Acknowledgements

This work was supported by the DIVERSAT project (Spanish Ministry of Science, Innovation and Universities RTI2018-098970-B-I00) and the Catalan Government BEG 2017SGR-378.

The main author is financially supported by a Basque Government predoctoral grant (Reference N°: PRE_2022_2_0127)

APPENDICES.

Appendix a. GPS positioning of the sampling locations

Location	Latitude	Longitude
L1: Malpica	43°21′07.4″N	08°49′52.2″W
L2: Cedeira	43°39′48.8″N	08°05′34.8″W
L3: Luarca	43°33′24.4″N	06°32′50.4″W
L4: Lastres	43°31′09.4″N	05°15′59.3″W
L5: San Vicente de la Barquera	43°24′06.0″N	04°23′59.4″W
L6: Somocuevas	43°28′15.1″N	03°56′28.1″W
L7: Kobaron	43°21′11.2″N	03°08′56.3″W
L8: Ea	43°23′18.3″N	02°34′57.7″W
L9: La Herradura	36°44′07.4″N	03°45′36.1″W
L10: Cabo Palos	37°38′08.3″N	00°41′17.5″W

Appendix b. Summer Sea Surface Temperature (SST) values for the sampling years and the two previous years for each location

	Summer SST (°C)						
Locations	2013	2014	2015	2017	2018	2019	2020
L1: Malpica	16.492	17.410	16.650	17.272	16.308	16.525	–
L2: Cedeira	17.120	17.686	17.046	17.504	15.889	16.980	–
L3: Luarca	18.528	19.130	18.872	19.110	18.190	18.370	–
L4: Lastres	19.827	20.490	19.862	19.919	20.109	20.058	–
L5: San Vicente	20.498	20.846	20.323	20.429	21.036	20.741	–
L6: Somocuevas	20.698	20.978	20.526	20.430	21.142	20.603	–
L7: Kobaron	21.160	21.287	20.777	20.946	21.764	20.997	–
L8: Ea	21.582	21.869	21.400	21.229	22.217	21.590	–
L9: La Herradura	22.999	21.716	22.400	–	23.279	22.738	23.303
L10: Cabo Palos	24.926	25.683	25.952	–	26.144	25.703	25.716

Appendix c. Mean cover (%) of the species contributing the most to the similarity within groups detected in the SIMPER routine for 2019–2020. L1: Malpica; L2: Cedeira; L3: Luarca; L4: Lastres; L5: San Vicente; L6: Somocuevas; L7: Kobaron; L8: Ea; L9: La Herradura; and L10: Cabo Palos

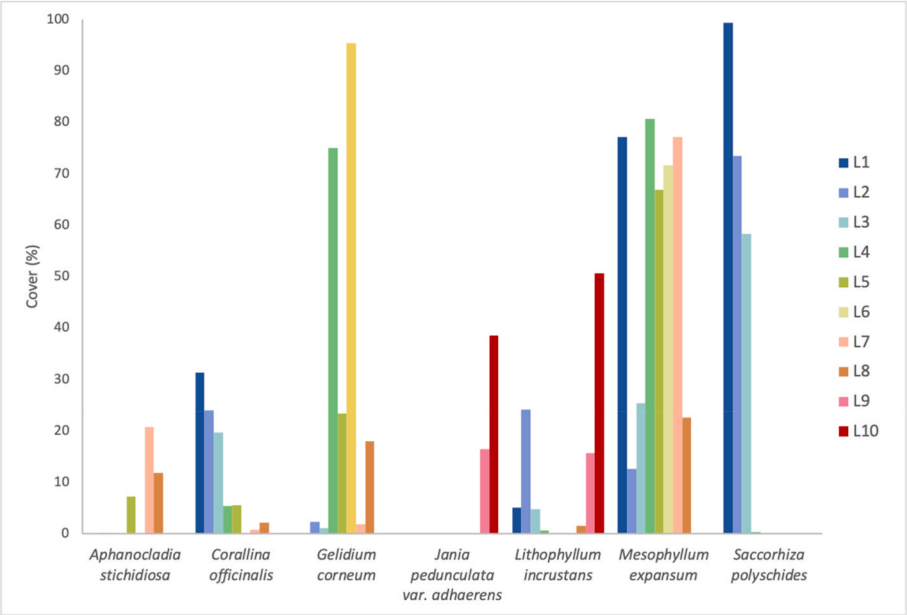

Appendix d. Mean cover (%) and contribution (%) of the taxa to the average similarity within each group according to the SIMPER routine. Only taxa with a contribution >4% to the average similarity of the group are included. a) 2015 and b) 2019–2020

SIMPER results - similarity percentage - species contributions					
a) 2015	Mean cover (%)	Contribution (%)	b) 2019	Mean cover (%)	Contribution (%)
Taxa list			Taxa list		
Group A - average similarity 60.90%- (L1, L2 & L3)			**Group A** - average similarity 62.47%- (L1, L2 & L3)		
Saccorhiza polyschides	68.13	16.42	*Saccorhiza polyschides*	77.04	20.22
Corallina officinalis	44.69	15.16	*Corallina officinalis*	24.94	10.72
Pterosiphonia complanata	11.65	6.07	*Mesophyllum expansum*	38.33	10.45
Chondracanthus teedei	6.34	5.00	*Hincksia* sp.	25.63	9.76
Jania squamata	10.56	4.77	*Lithophyllum incrustans*	11.25	5.42
Asparagopsis armata (*Falkenbergia rufolanosa* phase)	5.69	4.52			
Lithophyllum incrustans	27.40	4.33			
Group B - average similarity 56.51%- (L4, L5 & L6)			**Group B** - average similarity 67.14%- (L4 & L6)		
Gelidium corneum	69.18	21.25	*Gelidium corneum*	85.16	29.51
Mesophyllum expansum	65.10	21.02	*Mesophyllum expansum*	76.09	28.33
Plocamium cartilagineum	16.72	8.52	*Plocamium cartilagineum*	18.75	13.51
Cryptopleura ramosa	9.82	5.63	*Rhodymenia pseudopalmata*	3.52	4.06
Falkenbergia rufolanosa	15.67	4.29			
Group C -average similarity 60.32%- (L7 & L8)			**Group C** -average similarity 62.17%- (L5, L7 & L8)		
Mesophyllum expansum	64.69	18.58	*Mesophyllum expansum*	55.52	13.36
Aphanocladia stichidiosa	25.16	10.83	*Aphanocladia stichidiosa*	13.24	6.20
Zanardinia typus	10.16	5.67	*Zanardinia typus*	9.25	5.75
Codium decorticatum	13.69	5.16	*Gelidium corneum*	14.39	5.60
			Ellisolandia elongata	10.49	4.97
			Codium decorticatum	11.60	4.30
			Ceramium secundatum	5.05	4.24
			Asparagopsis armata (*Falkenbergia rufolanosa* phase)	4.67	4.01
Group D - average similarity 75.67%- (L9)			**Group D** - average similarity 63.68%- (L9 & L10)		
Halopteris scoparia	56.56	15.80	*Lithophyllum incrustans*	33.13	10.16
Mesophyllum expansum	38.75	15.42	*Jania pedunculata* var. *adhaerens*	27.44	9.43
Ellisolandia elongata	11.25	7.45	*Halopteris scoparia*	19.88	9.37
Lithophyllum incrustans	8.44	6.89	*Halopteris filicina*	7.06	5.84

(*continued on next page*)

(*continued*)

SIMPER results - similarity percentage - species contributions					
a) 2015	Mean cover (%)	Contribution (%)	b) 2019	Mean cover (%)	Contribution (%)
Taxa list			Taxa list		
Zanardinia typus	5.66	5.63	*Peyssonnelia atropurpurea*	4.70	4.69
Halopteris filicina	6.16	5.03			
Group E - average similarity 56.04%- (L10)					
Padina pavonica	49.06	19.98			
Lithophyllum incrustans	14.69	10.68			
Caulerpa racemosa	2.94	5.16			
Wrangelia penicillata	4.03	4.43			

*Appendix e. Thermal optimum (TO) and average abundance in percent cover of the taxa identified for each locality and year (2015–2019/20). *Cladostephus spongiosus is now recognized as two different taxa: Cladostephus spongiosus s.s. and Cladostephus hirsutus. ** Vertebrata fruticulosa is now recognized as two different taxa: Vertebrata fruticulosa s.s. and Vertebrata martensiana*

	TO	2015	2019	2015	2019	2015	2019	2015	2019	2015	2019	2015	2019	2015	2019	2015	2019	2015	2020	2015	2020
		MAL	MAL	CED	CED	LUA	LUA	LAS	LAS	SVB	SVB	SOM	SOM	KOB	KOB	EA	EA	HER	HER	CAB	CAB
Acrosorium ciliolatum	14.56	4.06	0.63	1.75	0.44	6.50	0.44	1.06	0.72	2.16	1.91	1.28	1.28	0.53	0.19	2.59	0.38	0.06	0.00	0.00	0.00
Acrothamnion preissii	15.81	0.00	0.00	0.00	0.00	0.00	0.00	0.00	0.00	0.00	0.00	0.00	0.00	0.00	0.00	0.00	0.00	0.00	0.13	0.00	0.31
Aglaothamnion pseudobyssoides	10.43	0.00	0.00	0.00	0.00	0.16	0.09	0.28	0.00	10.22	0.00	0.00	0.00	5.75	0.00	0.00	0.00	0.00	0.00	0.00	0.00
Aglaothamnion tenuissimum	14.72	0.00	0.00	0.00	0.00	0.00	0.00	0.00	0.00	0.03	0.28	0.00	0.00	0.31	0.00	0.09	0.03	0.00	0.00	0.00	0.00
Ahnfeltiopsis devoniensis	12.22	0.00	0.00	0.00	0.00	0.00	0.00	2.38	0.03	0.00	0.00	0.00	0.00	0.00	0.00	0.00	0.00	0.00	0.00	0.00	0.00
Amphiroa kuetzingiana	16.77	0.00	0.00	0.00	0.00	0.00	0.00	0.00	0.00	0.00	0.00	0.00	0.00	0.00	0.00	0.00	0.00	0.00	0.06	0.00	0.00
Amphiroa rigida	19.08	0.00	0.00	0.00	0.00	0.00	0.00	0.00	0.00	0.00	0.00	0.00	0.00	0.00	0.13	0.00	0.00	1.25	4.69	3.84	2.25
Anadyomene stellata	19.04	0.00	0.00	0.00	0.00	0.00	0.00	0.00	0.00	0.00	0.00	0.00	0.00	0.00	0.00	0.00	0.00	0.00	0.00	1.38	0.06
Anotrichium furcellatum	17.28	0.00	0.00	0.00	0.06	0.00	0.00	0.00	0.22	0.00	2.34	0.00	0.00	0.00	0.00	0.06	0.00	0.00	0.00	0.00	0.00
Anotrichium tenue	19.91	0.00	0.00	0.00	0.00	0.00	0.00	0.00	0.00	0.00	0.00	0.00	0.00	0.00	0.00	0.00	0.00	0.06	0.03	0.13	0.09
Antithamnion amphigeneum	16.78	0.00	0.00	0.00	0.00	0.00	0.00	0.00	0.00	0.03	0.00	0.00	0.00	0.00	0.00	0.00	0.00	0.00	0.00	0.00	0.00
Antithamnion cruciatum	15.54	0.00	0.00	0.00	0.00	0.00	0.00	0.00	0.00	0.00	0.00	0.00	0.00	0.00	0.00	0.00	0.00	0.09	0.06	0.00	0.00
Antithamnion decipiens	22.01	0.00	0.00	0.00	0.00	0.00	0.00	0.00	0.00	0.00	0.00	0.00	0.00	0.00	0.00	0.00	0.00	0.00	0.00	0.13	0.00
Antithamnion densum	7.45	0.00	0.00	0.00	0.06	0.00	0.00	0.00	0.00	0.00	0.00	0.00	0.00	0.00	0.00	0.00	0.00	0.00	0.00	0.00	0.00
Antithamnion heterocladum	13.66	0.00	0.00	0.00	0.00	0.00	0.00	0.00	0.00	0.00	0.00	0.00	0.00	0.00	0.00	0.00	0.00	0.00	0.00	0.00	0.00
Antithamnion hubbsii	19.54	0.00	0.00	0.00	0.00	0.00	0.00	0.00	0.00	0.09	0.00	0.00	0.00	0.00	0.00	0.00	0.00	0.00	0.00	0.00	0.00
Antithamnionella spirographidis	11.92	0.00	0.00	0.00	0.00	0.00	0.00	0.00	0.38	0.00	0.00	0.00	0.00	0.00	0.00	0.00	0.00	0.00	0.00	0.00	0.00
Antithamnionella ternifolia	11.92	0.13	0.00	0.03	0.03	0.00	0.00	0.34	0.00	2.84	0.06	0.13	0.00	0.00	0.00	0.06	0.00	0.00	0.00	0.00	0.00
Aphanocladia stichidiosa	17.21	0.00	0.00	0.00	0.06	0.00	0.16	0.00	0.00	0.00	7.22	0.00	0.00	15.94	20.63	34.38	11.88	0.00	0.00	0.00	0.00
Apoglossum ruscifolium	11.12	0.03	0.03	0.25	0.38	0.13	0.41	0.22	0.53	0.28	0.38	1.19	1.75	0.06	0.25	0.59	0.38	0.00	0.03	0.00	0.00
Asparagopsis armata	12.03	14.81	0.34	5.00	5.16	3.94	1.13	28.75	4.94	21.97	7.03	0.00	0.19	24.03	5.91	0.97	4.19	3.13	0.03	0.69	0.00
Asparagopsis taxiformis	19.47	0.00	0.00	0.00	0.00	0.00	0.00	0.00	0.00	0.00	0.00	0.00	0.00	0.00	0.00	0.00	0.00	6.16	15.09	0.00	0.78
Bonnemaisonia asparagoides	10.49	0.00	0.00	0.00	0.00	0.00	0.09	0.72	0.00	0.00	0.00	0.00	0.09	2.81	2.47	0.66	0.22	0.00	0.00	0.00	0.00
Bonnemaisonia clavata	12.51	0.00	0.00	0.00	0.00	0.00	0.00	0.00	0.00	0.00	0.00	0.00	0.00	0.00	0.00	0.00	0.00	0.00	0.00	0.03	0.00
Bonnemaisonia hamifera	12.20	1.72	0.00	0.00	0.00	0.00	0.00	0.00	0.00	0.19	0.06	13.75	0.00	10.31	0.00	1.25	0.63	0.00	0.03	0.00	0.00
Bornetia secundiflora	11.62	0.00	0.00	0.00	0.03	0.03	0.06	0.00	0.28	0.03	0.63	0.00	0.00	0.00	0.00	0.00	0.00	0.00	0.00	0.00	0.00
Botryocladia botryoides	17.78	0.00	0.00	0.00	0.00	0.00	0.00	0.00	0.00	0.00	0.00	0.00	0.00	0.00	0.00	0.00	0.00	0.00	0.00	0.03	0.88
Bryopsis cupressina	18.69	0.00	0.00	0.00	0.00	0.00	0.00	0.00	0.00	0.00	0.00	0.00	0.00	0.00	0.00	0.00	0.00	0.00	0.41	0.00	0.00
Bryopsis hypnoides	13.77	0.00	0.00	0.00	0.00	0.00	0.00	0.00	0.00	0.00	0.00	0.00	0.00	0.22	0.38	0.03	0.00	0.03	0.00	0.00	0.00
Bryopsis pennata	22.43	0.00	0.00	0.00	0.00	0.00	0.00	0.00	0.00	0.00	0.00	0.00	0.00	0.00	0.00	0.00	0.00	0.16	0.00	0.00	0.00
Bryopsis plumosa	16.82	0.00	0.00	0.00	0.00	0.00	0.00	0.00	0.00	0.00	0.00	0.00	0.00	0.22	0.97	0.19	0.00	0.00	0.00	0.00	0.00
Calliblepharis ciliata	10.44	0.00	0.00	0.69	0.31	0.09	0.00	0.31	0.22	0.31	0.03	3.19	0.00	0.00	0.00	0.00	0.00	0.00	0.00	0.00	0.00
Callithamnion corymbosum	14.92	0.00	0.00	0.00	0.00	0.00	0.19	0.00	0.00	0.00	0.00	0.00	0.00	0.00	0.00	0.00	0.00	0.00	0.03	0.00	0.47
Callithamnion granulatum	11.46	0.00	0.00	0.00	0.03	0.00	0.00	0.00	0.00	0.00	0.00	0.00	0.00	0.00	0.00	0.00	0.00	0.00	0.00	0.00	0.00
Callithamnion tetragonum	10.87	0.03	0.00	0.00	0.00	0.00	0.00	0.16	0.06	0.16	0.00	0.00	0.00	0.00	0.00	0.00	0.00	0.00	0.00	0.00	0.00
Carpomitra costata	13.88	0.00	0.00	0.00	0.00	0.00	0.03	0.00	0.00	0.00	0.00	0.00	0.00	0.00	0.00	0.00	0.00	0.00	0.00	0.00	0.00
Caulacanthus ustulatus	16.03	0.00	0.00	0.00	0.00	0.00	0.00	0.00	0.00	0.00	0.00	0.00	0.00	0.00	0.00	0.00	0.00	0.09	0.00	0.06	0.03
Caulerpa racemosa	20.26	0.00	0.00	0.00	0.00	0.00	0.00	0.00	0.00	0.00	0.00	0.00	0.00	0.00	0.00	0.00	0.00	0.00	0.00	2.94	3.16
Centroceras clavulatum	18.03	0.00	0.00	0.00	0.00	0.00	0.03	0.00	0.00	0.00	0.00	0.00	0.00	0.00	0.03	0.00	0.06	0.38	0.28	0.00	0.00
Ceramium botryocarpum	10.49	0.00	0.00	0.00	0.00	0.00	0.00	0.00	0.00	0.03	0.00	0.00	0.00	0.00	0.00	0.00	0.00	0.00	0.00	0.00	0.00
Ceramium ciliatum	11.29	0.00	0.00	0.03	0.00	0.00	0.28	0.03	0.00	0.00	0.00	0.00	0.00	0.19	3.13	2.53	3.22	0.00	0.00	4.75	0.00
Ceramium cingulatum	20.64	0.00	0.00	0.00	0.00	0.00	0.00	0.00	0.00	0.00	0.00	0.00	0.00	0.00	0.00	0.00	0.00	0.03	0.09	0.00	0.38
Ceramium circinatum	13.13	0.00	0.00	0.00	0.00	0.00	0.00	0.00	0.00	0.00	0.00	0.00	0.00	0.00	1.88	0.00	0.84	0.03	0.22	0.50	0.28
Ceramium codii	19.33	0.00	0.00	0.00	0.00	0.00	0.00	0.00	0.00	0.00	0.00	0.00	0.00	0.00	0.00	0.00	0.00	0.28	1.09	0.34	0.81
Ceramium diaphanum	15.70	0.00	0.00	0.00	0.09	0.00	0.28	0.00	0.09	0.00	0.00	0.00	0.00	0.00	0.00	0.00	0.47	0.00	0.00	0.00	0.00
Ceramium echionotum	11.46	0.00	0.00	0.00	0.00	0.19	0.19	0.09	0.00	0.25	0.00	0.00	0.00	0.56	7.69	2.50	3.97	0.13	0.03	0.00	0.03
Ceramium secundatum	11.35	0.06	0.00	0.09	0.09	0.31	0.25	0.09	0.00	0.09	6.41	0.00	0.00	0.22	5.44	2.00	3.31	0.00	0.00	0.00	0.00
Champia parvula	16.66	0.00	0.00	0.00	0.00	0.03	0.16	0.91	0.00	0.13	0.44	0.00	0.00	0.16	0.31	2.50	0.41	0.53	1.63	0.59	0.81
Chondracanthus acicularis	17.42	0.00	0.00	0.00	0.03	0.00	0.13	0.00	0.06	0.00	0.00	0.00	0.00	0.00	0.00	0.00	0.00	0.13	0.13	0.00	0.00
Chondracanthus teedei	15.24	9.50	2.63	6.25	3.41	3.28	1.34	3.25	0.06	0.34	0.16	0.00	0.00	0.00	0.00	0.00	0.00	0.00	0.00	0.00	0.00
Chondria capillaris	16.63	0.00	0.00	0.00	0.03	0.00	0.22	0.00	0.00	0.00	0.00	0.00	0.00	0.00	0.00	0.00	0.00	0.00	0.00	0.16	0.00

(*continued on next page*)

(*continued*)

	TO	2015	2019	2015	2019	2015	2019	2015	2019	2015	2019	2015	2019	2015	2019	2015	2019	2015	2020	2015	2020
Chondria coerulescens	12.30	0.00	0.00	1.19	1.44	0.19	0.19	0.00	0.00	0.00	0.00	0.00	0.00	0.00	0.00	0.00	0.00	0.00	0.00	0.09	0.03
Chondria scintillans	9.22	0.00	0.00	0.00	0.00	2.94	0.63	0.00	0.00	0.00	0.00	0.00	0.00	0.00	0.00	0.00	0.00	0.00	0.00	0.00	0.00
Chrysymenia ventricosa	17.68	0.00	0.00	0.00	0.00	0.00	0.00	0.00	0.00	0.00	0.00	0.00	0.00	0.00	0.00	0.06	0.00	0.00	0.00	0.00	0.00
Chylocladia verticillata	10.53	0.00	0.00	0.00	0.00	0.00	0.03	0.00	0.00	0.00	0.00	0.00	0.00	0.00	0.00	0.00	0.00	0.00	0.59	0.03	0.00
Cladophora coelothrix	16.54	0.00	0.00	0.00	0.00	0.00	0.00	0.00	0.00	0.00	0.00	0.00	0.00	0.00	0.00	0.00	0.00	0.34	0.00	0.66	0.41
Cladophora hutchinsiae	11.74	0.00	0.25	0.00	0.00	0.00	0.00	0.00	0.00	0.00	0.13	0.00	0.00	1.47	0.50	0.56	0.41	0.00	0.06	0.00	0.00
Cladophora lehmanniana	16.97	0.00	0.00	0.00	0.00	0.13	0.03	0.06	0.00	0.00	0.00	0.00	0.00	0.00	0.00	0.06	0.00	0.00	0.00	0.00	0.06
Cladophora prolifera	17.51	0.00	0.00	0.00	0.00	0.00	0.00	0.00	0.00	6.56	0.50	0.00	0.00	0.50	0.59	1.94	0.59	0.06	0.88	0.75	0.03
Cladophora rupestris	7.95	0.00	0.00	0.00	0.00	0.00	0.00	0.00	0.00	0.00	2.72	0.00	0.00	0.00	1.00	0.00	0.00	0.00	0.00	0.00	0.00
Cladophora sericea	11.56	0.00	0.00	0.00	0.00	0.00	0.00	0.00	0.00	0.00	0.00	0.00	0.00	0.00	0.00	0.00	0.00	0.00	0.00	0.28	0.00
Cladophora socialis	21.74	0.00	0.00	0.00	0.00	0.00	0.00	0.00	0.00	0.00	0.00	0.00	0.00	0.00	0.00	0.00	0.00	0.00	0.00	1.81	0.00
*Cladostephus spongiosus**	11.00	0.13	0.00	2.31	0.31	4.50	0.50	0.31	0.00	0.25	0.28	0.00	0.00	0.63	0.00	2.25	1.94	0.00	0.00	0.00	3.06
Codium adhaerens	16.40	1.25	0.19	0.00	0.00	0.00	0.13	0.00	0.00	0.00	0.00	0.00	0.00	0.00	0.00	0.00	0.00	0.00	0.00	0.03	0.00
Codium bursa	12.53	0.00	0.00	0.00	0.00	0.00	0.00	0.00	0.00	0.00	0.00	0.00	0.00	0.00	0.00	0.00	0.00	0.00	0.03	0.00	0.00
Codium decorticatum	18.16	2.63	0.00	4.19	0.38	2.19	0.00	0.38	0.00	0.84	6.63	0.00	0.06	24.88	26.06	2.50	2.13	0.00	0.00	0.00	0.00
Codium fragile	14.30	0.00	0.13	0.00	0.00	2.03	0.00	2.28	0.00	0.00	0.31	0.00	0.00	0.00	1.63	0.00	0.00	0.00	0.00	0.00	0.00
Codium tomentosum	16.00	0.00	0.00	0.00	0.00	0.00	0.00	0.00	0.00	0.00	0.31	0.00	0.00	0.00	0.00	0.00	0.00	0.00	0.00	0.00	0.00
Codium vermilara	10.69	0.00	0.22	0.00	4.00	0.00	0.91	0.00	0.00	0.00	0.31	0.00	0.00	0.00	4.06	0.06	0.94	0.00	0.00	0.34	0.00
Colpomenia peregrina	11.96	0.00	0.00	0.00	0.06	0.00	0.00	0.00	0.00	0.00	0.16	0.00	0.00	3.84	3.50	0.94	0.00	0.00	0.22	0.00	0.00
Colpomenia sinuosa	16.18	0.00	0.00	0.00	0.00	0.00	0.00	0.00	0.03	0.03	0.09	0.00	0.00	0.00	0.31	0.00	0.00	0.03	0.06	0.00	0.03
Compsothamnion thuioides	12.57	0.00	0.00	0.00	0.00	0.00	0.00	0.00	0.00	0.00	0.28	0.00	0.00	0.00	0.38	0.00	0.00	0.06	0.00	0.00	0.00
Corallina officinalis	15.20	52.19	31.25	40.00	23.88	41.88	19.69	8.16	5.41	1.81	5.44	0.00	0.00	0.00	0.72	0.00	2.19	0.00	0.00	0.00	0.00
Crouania attenuata	16.71	0.00	0.00	0.53	0.34	0.22	0.38	1.28	0.00	0.94	0.34	0.00	0.00	0.00	0.31	0.31	0.25	0.06	0.19	0.13	0.41
Cryptonemia palmetta	11.06	0.00	0.00	0.00	0.00	0.00	0.00	0.00	0.19	0.00	0.00	0.00	0.00	0.00	0.00	0.00	0.09	0.00	0.00	0.03	0.00
Cryptopleura ramosa	12.26	0.88	1.00	0.06	0.56	7.81	0.50	2.81	1.50	4.16	1.47	22.50	0.03	0.00	0.13	0.00	0.47	0.00	0.00	0.00	0.00
Cutleria adspersa	16.82	0.00	0.00	0.00	0.00	0.00	0.00	0.00	0.00	0.00	0.00	0.00	0.00	0.00	0.09	0.00	0.00	0.00	0.00	0.00	0.00
Cutleria multifida	12.39	0.00	0.00	0.00	0.94	0.00	0.00	0.00	0.00	0.00	0.00	0.00	0.00	0.00	0.00	0.00	0.00	0.44	0.38	0.00	0.28
Cystoseira compressa	16.92	0.00	0.00	0.00	0.00	0.00	0.00	0.00	0.00	0.00	0.00	0.00	0.00	0.00	0.00	0.00	0.00	0.06	0.03	0.44	0.00
Dasya corymbifera	17.24	0.00	0.00	0.00	0.00	0.00	0.06	0.00	0.00	0.00	0.00	0.00	0.00	0.00	0.00	0.00	0.00	0.06	0.00	0.16	0.38
Dasya hutchinsiae	11.71	0.00	0.00	0.00	0.09	0.03	0.00	1.44	0.06	0.88	0.97	0.00	0.00	0.00	0.00	0.00	0.00	0.00	0.00	0.00	0.00
Dasya ocellata	16.80	0.03	0.00	0.03	0.00	0.47	0.00	0.63	0.00	0.06	1.97	0.00	0.00	0.47	4.38	0.81	1.53	0.00	0.00	0.09	0.00
Dasya rigidula	19.84	0.00	0.00	0.00	0.00	0.00	0.00	0.00	0.00	0.00	0.00	0.00	0.00	0.00	0.00	0.00	0.00	0.03	0.00	0.19	0.31
Dasycladus vermicularis	18.99	0.00	0.00	0.00	0.00	0.00	0.00	0.00	0.00	0.00	0.00	0.00	0.00	0.00	0.00	0.00	0.00	0.00	0.00	0.00	0.03
Deltalsia parasitica	11.85	0.00	0.00	0.00	0.00	0.06	0.00	0.03	0.00	0.28	0.13	0.00	0.00	0.16	0.31	1.22	0.13	0.00	0.00	0.00	0.00
Derbesia tenuissima	16.39	0.00	0.00	0.03	0.00	0.00	0.00	0.00	0.06	0.34	0.00	0.00	0.00	0.03	0.06	0.19	0.00	0.00	0.84	0.00	0.00
Desmarestia ligulata	12.42	1.13	0.06	0.63	0.44	0.00	0.13	0.31	0.00	0.00	0.00	0.00	0.00	2.59	0.00	0.00	0.00	0.00	0.00	0.00	0.00
Dictyopteris polypodioides	13.66	0.31	0.06	0.22	0.75	0.00	0.16	0.00	0.13	0.00	0.00	0.00	0.00	0.00	0.00	0.00	0.00	0.06	0.41	0.22	0.56
Dictyota cyanoloma	14.36	0.00	0.00	0.00	0.00	0.00	0.00	0.00	0.00	0.00	0.00	0.00	0.00	0.00	0.00	0.00	0.00	0.00	0.09	0.00	0.00
Dictyota dichotoma	15.98	1.63	0.31	0.50	0.88	0.00	0.72	0.59	7.13	7.28	0.00	0.69	0.00	0.00	0.22	1.25	1.09	0.81	0.59	0.63	0.25
Dictyota dichotoma var. *intricata*	15.35	0.00	0.03	0.00	0.09	0.00	0.06	0.00	0.16	0.00	4.31	0.00	0.00	0.00	0.00	0.00	0.00	0.00	0.00	0.00	0.00
Dictyota implexa	17.76	0.00	0.00	0.00	0.00	0.00	0.00	0.00	0.00	0.00	0.00	0.00	0.00	0.00	0.00	0.00	0.00	0.00	1.38	0.00	1.03
Dictyota spiralis	11.55	0.00	0.00	0.00	0.19	0.00	0.22	0.00	0.06	0.00	0.03	0.00	0.00	0.00	0.00	0.00	0.00	0.00	0.00	0.41	0.00
Dumontia contorta	9.01	0.00	0.00	1.13	0.13	0.06	0.00	0.00	0.00	0.00	0.00	0.00	0.00	0.00	0.00	0.00	0.00	0.00	0.00	0.00	0.00
Ellisolandia elongata	15.51	0.31	1.88	0.31	2.72	5.00	16.06	14.25	2.03	12.56	15.72	0.00	0.00	0.47	2.06	9.44	13.69	11.25	8.94	1.16	0.97
Ericaria selaginoides	11.59	0.00	0.00	0.00	0.00	0.00	0.00	0.63	0.00	0.00	3.31	0.00	0.00	0.00	0.00	0.63	0.00	0.00	2.94	0.00	0.00
Erythroglossum laciniatum	12.47	0.00	0.00	0.00	0.03	0.00	0.00	0.00	0.03	0.00	0.00	0.00	0.00	0.00	0.00	0.00	0.00	0.00	0.00	0.00	0.00
Gaillona gallica	12.62	0.00	0.00	0.00	0.03	0.00	0.00	0.00	0.00	0.00	0.00	0.00	0.00	0.03	0.00	0.00	0.00	0.00	0.00	0.00	0.00
Gastroclonium ovatum	11.28	0.00	0.00	0.00	0.00	0.03	0.00	0.00	0.00	0.00	0.00	0.00	0.00	0.00	0.00	0.13	0.00	0.00	0.00	0.00	0.00
Gastroclonium reflexum	12.03	0.00	0.00	0.00	0.00	0.00	0.00	0.00	0.00	0.00	0.00	0.00	0.00	0.00	0.00	0.13	0.00	0.00	0.00	0.00	0.00
Gayliella flaccida	17.06	0.00	0.00	0.47	0.16	6.94	0.00	15.13	0.06	0.56	0.13	0.00	0.00	0.25	1.59	0.66	0.38	0.28	1.84	1.53	0.72
Gelidium attenuatum	15.42	0.09	0.00	1.72	0.00	6.88	0.00	5.94	0.00	0.00	0.00	0.00	0.00	0.00	0.00	0.00	0.00	0.00	0.22	0.00	0.00
Gelidium corneum	12.48	0.00	0.00	0.00	2.23	0.00	1.09	54.38	75.00	59.09	23.38	94.06	95.31	0.00	1.78	21.75	18.00	0.00	0.00	0.00	0.00
Gelidium pusillum	17.06	0.00	0.00	0.00	0.00	0.00	0.00	0.00	0.00	0.00	0.03	0.00	0.00	0.00	0.00	0.00	0.00	0.25	1.31	0.25	0.94
Gelidium spinosum	13.06	0.00	0.25	0.00	0.09	0.00	0.25	0.00	0.13	0.00	0.00	0.03	0.00	0.28	4.53	4.59	0.38	0.00	0.13	0.00	0.00
Gigartina pistillata	14.86	0.31	0.06	0.25	1.81	0.94	0.34	0.44	1.66	0.00	0.13	0.00	0.00	0.00	0.00	0.00	0.03	0.00	0.00	0.00	0.00
Gongolaria baccata	11.54	0.00	0.00	3.44	0.44	3.44	0.88	6.25	0.88	0.69	2.88	0.00	0.00	0.00	0.00	0.00	0.50	0.00	0.00	0.00	0.00
Grateloupia filicina	16.44	0.00	0.00	0.00	0.00	0.00	0.00	0.00	0.00	0.00	0.00	0.00	0.00	0.00	0.00	0.00	0.00	0.00	0.00	0.69	0.00
Griffithsia schousboei	19.63	0.00	0.00	0.00	0.00	0.00	0.00	0.00	0.00	0.00	0.00	0.00	0.00	0.00	0.00	0.00	0.00	0.03	0.00	0.00	0.03
Gymnogongrus crenulatus	12.03	1.25	3.25	11.94	3.44	0.81	0.06	0.00	0.13	0.06	0.09	0.00	0.00	0.00	0.00	0.00	0.00	0.00	0.00	0.00	0.00
Halimeda tuna	18.94	0.00	0.00	0.00	0.00	0.00	0.00	0.00	0.00	0.00	0.00	0.00	0.00	0.00	0.00	0.00	0.00	0.00	0.00	0.03	0.00
Halopithys incurva	13.00	0.00	0.00	0.00	0.00	0.00	0.00	0.00	0.00	0.00	0.00	0.00	0.00	0.00	0.06	0.06	0.00	0.00	0.00	0.00	0.00
Halopteris filicina	13.21	0.06	0.00	0.06	0.38	0.22	0.38	0.00	0.13	0.03	0.00	0.00	0.00	0.00	0.00	0.00	0.06	6.16	7.53	3.09	6.59
Halopteris scoparia	12.48	1.41	0.00	0.06	0.28	2.44	0.63	0.47	0.06	0.34	0.00	0.00	0.00	1.69	1.19	2.72	1.19	56.56	19.44	5.59	20.31
Halurus equisetifolius	10.46	3.63	1.00	3.50	1.04	3.03	0.97	0.72	1.09	0.44	1.25	0.00	0.00	0.00	0.00	0.00	1.16	0.00	0.00	0.00	0.00
Herposiphonia secunda	17.67	0.00	0.00	0.00	0.00	0.00	0.00	0.00	0.00	0.00	0.00	0.00	0.00	0.00	0.69	0.00	0.00	0.47	0.66	0.97	2.19
Herposiphonia tenella	18.91	0.00	0.00	0.00	0.00	0.00	0.19	0.91	0.09	0.00	0.00	0.00	0.00	0.00	0.00	0.06	2.59	0.00	0.00	0.00	0.00
Heterosiphonia crispella	19.52	0.00	0.00	0.00	0.00	0.00	0.00	0.00	0.00	0.00	0.00	0.00	0.00	0.00	0.00	0.00	0.00	0.53	0.50	0.22	0.84
Heterosiphonia plumosa	9.58	0.19	0.25	5.19	13.75	1.91	1.00	0.03	0.22	0.00	0.38	0.00	0.00	0.00	0.00	0.00	0.72	0.00	0.00	0.00	0.00
Hildenbrandia rubra	14.21	0.00	0.00	0.00	0.00	0.00	0.00	0.00	0.00	0.00	0.00	0.00	0.00	0.00	0.00	0.00	0.00	0.00	0.00	0.00	0.13
Hypoglossum hypoglossoides	16.42	0.03	0.00	0.19	0.09	0.03	0.00	0.09	0.00	0.00	0.00	0.00	0.00	0.00	0.00	0.00	0.00	0.34	0.34	0.03	0.00
Jania pedunculata var. *adhaerens*	22.07	0.00	0.00	0.00	0.00	0.00	0.00	0.00	0.00	0.00	0.00	0.00	0.00	0.00	0.00	0.00	0.00	0.00	16.44	0.00	38.44
Jania longifurca	16.75	0.00	0.00	0.00	0.06	0.00	0.25	0.00	0.00	0.00	0.00	0.00	0.00	0.00	0.38	0.00	0.13	0.00	1.38	0.00	0.00
Jania rubens	15.59	0.06	0.00	0.13	0.00	2.53	0.16	3.53	0.25	0.91	1.63	0.00	0.00	0.81	6.22	7.50	5.13	0.00	1.13	0.25	0.34
Jania squamata	16.75	10.94	0.00	1.38	0.06	19.38	12.81	4.25	2.94	0.00	4.78	0.00	0.00	0.00	0.16	0.00	1.28	0.00	1.66	0.00	0.00

(*continued on next page*)

(*continued*)

	TO	2015	2019	2015	2019	2015	2019	2015	2019	2015	2019	2015	2019	2015	2019	2015	2019	2015	2020	2015	2020
Jania virgata	14.97	0.00	0.00	0.00	0.00	0.00	0.00	0.00	0.00	0.00	0.00	0.00	0.00	0.00	0.00	0.00	0.00	0.44	0.00	6.81	0.16
Kallymenia reniformis	7.45	0.03	0.00	0.03	0.00	0.03	0.00	0.22	0.00	0.41	0.00	0.13	0.00	0.00	0.00	0.00	0.00	0.00	0.00	0.00	0.00
Laminaria ochroleuca	13.25	2.63	0.00	0.00	0.50	0.00	0.00	0.00	0.00	0.00	0.00	0.00	0.00	0.00	0.00	0.00	0.00	0.00	0.00	0.00	0.00
Laurencia minuta	19.01	0.00	0.00	0.00	0.00	0.00	0.00	0.00	0.00	0.00	0.00	0.00	0.00	0.00	0.00	0.00	0.00	0.00	0.19	0.00	0.50
Laurencia obtusa	17.12	0.00	0.00	0.00	0.00	0.00	0.00	0.00	0.00	0.00	0.00	0.00	0.00	0.00	0.00	0.00	0.00	0.19	0.00	0.47	0.00
Leptosiphonia brodiei	9.27	0.00	0.00	0.00	0.00	0.00	0.00	0.00	0.00	0.00	0.00	0.00	0.00	0.00	0.00	0.00	0.00	0.00	0.00	0.06	0.00
Liagora viscida	14.24	0.00	0.00	0.00	0.00	0.00	0.00	0.00	0.00	0.00	0.00	0.00	0.00	0.00	0.00	0.31	0.63	0.00	0.00	0.00	0.00
Lithophyllum incrustans	16.40	12.19	5.00	70.00	24.06	0.00	4.69	0.00	0.63	0.00	0.00	0.00	0.00	0.13	0.00	0.38	1.50	8.44	15.63	14.69	50.63
Lobophora variegata	19.88	0.00	0.00	0.00	0.00	0.00	0.00	0.00	0.00	0.00	0.00	0.00	0.00	0.00	0.00	0.00	0.00	0.06	0.00	0.44	0.03
Lomentaria articulata	10.57	0.00	0.00	0.00	0.00	0.00	0.13	0.00	0.06	0.00	0.00	0.00	0.00	0.00	0.00	0.00	0.00	0.00	0.00	0.00	0.00
Lomentaria chylocladiella	16.11	0.00	0.00	0.00	0.00	0.00	0.00	0.00	0.00	0.00	0.00	0.00	0.00	0.00	0.00	0.00	0.00	0.06	0.00	0.00	0.00
Lomentaria clavellosa	10.79	0.00	0.00	0.00	0.00	0.00	0.00	0.00	0.00	0.00	0.03	0.00	0.00	0.09	0.00	0.47	0.00	0.00	0.00	0.00	0.00
Lomentaria verticillata	13.66	0.00	0.00	0.00	0.00	0.00	0.00	0.00	0.00	0.00	0.00	0.00	0.00	0.00	0.00	0.00	0.00	0.09	0.00	0.00	0.00
Lophocladia lallemandii	19.85	0.00	0.00	0.00	0.00	0.00	0.00	0.00	0.00	0.00	0.00	0.00	0.00	0.00	0.00	0.00	0.00	0.03	0.16	1.81	1.47
Lophosiphonia obscura	17.17	0.00	0.00	0.00	0.00	0.00	0.00	0.00	0.00	0.00	0.00	0.00	0.00	0.00	0.00	0.00	0.00	0.03	0.03	0.47	0.13
Lychaete pellucida	13.98	0.00	0.00	0.00	0.03	0.00	0.00	0.44	0.16	0.16	0.66	0.22	0.28	5.00	1.47	2.63	0.53	0.09	0.00	0.31	0.03
Meredithia microphylla	11.07	0.00	0.00	0.00	0.00	0.00	0.00	0.00	0.00	0.06	0.06	0.00	0.00	0.00	0.00	0.00	0.00	0.00	0.00	0.00	0.00
Mesophyllum expansum	16.92	12.81	77.19	0.00	12.50	26.56	25.31	75.00	80.63	64.06	66.88	56.25	71.56	79.69	77.19	49.69	22.50	38.75	31.56	0.00	0.00
Metacallophyllis laciniata	10.38	0.03	0.69	0.94	3.31	0.00	0.00	0.00	0.06	0.00	0.00	0.06	0.00	0.00	0.00	0.00	0.00	0.00	0.00	0.00	0.00
Microcladia glandulosa	7.29	0.00	0.00	0.06	0.06	2.91	1.06	5.84	0.03	0.50	0.38	0.00	0.00	6.16	0.34	2.22	4.47	0.00	0.00	0.00	0.00
Monosporus pedicellatus	15.72	0.00	0.00	0.00	0.00	0.00	0.00	0.00	0.00	0.00	0.03	0.00	0.00	0.00	0.00	0.00	0.00	0.00	0.00	0.00	0.00
Nitophyllum micropunctatum	15.52	0.00	0.00	0.00	0.00	0.00	0.00	0.00	0.00	0.00	0.00	0.00	0.00	0.00	0.00	0.00	0.00	0.00	0.00	0.19	0.00
Nitophyllum punctatum	9.60	0.13	0.00	0.03	0.13	0.00	0.03	0.00	0.00	0.00	0.00	0.03	0.00	0.00	0.00	0.47	0.19	0.00	0.50	0.19	0.06
Osmundea pinnatifida	15.65	0.00	0.00	0.00	0.00	0.00	0.00	0.00	0.00	0.00	0.00	0.00	0.00	0.00	0.00	0.00	0.00	0.09	0.00	0.00	0.00
Padina pavonica	17.75	0.00	0.00	0.00	0.00	0.00	0.00	0.00	0.00	0.00	0.00	0.00	0.00	0.00	0.00	0.00	0.00	0.03	0.00	49.06	25.00
Parvocaulis parvulus	21.69	0.00	0.00	0.00	0.00	0.00	0.00	0.00	0.00	0.00	0.00	0.00	0.00	0.00	0.00	0.00	0.00	0.00	0.00	0.34	0.06
Petalonia fascia	12.99	0.00	0.00	0.00	0.00	0.00	0.00	0.00	0.00	0.00	0.00	0.00	0.00	0.00	0.03	0.00	0.00	0.00	0.00	0.00	0.00
Peyssonnelia atropurpurea	12.23	0.00	0.06	0.00	7.16	1.25	0.44	1.25	0.03	0.47	2.50	3.97	0.59	0.59	1.31	1.03	0.16	1.59	4.91	0.72	4.50
Peyssonnelia rubra	18.92	5.94	0.00	0.00	0.00	0.00	0.00	0.00	0.31	0.00	0.00	0.00	0.00	0.00	0.00	0.00	0.00	0.00	0.22	0.00	0.00
Peyssonnelia squamaria	13.44	0.00	0.00	0.00	0.00	0.00	0.00	0.00	0.00	0.00	0.59	0.00	0.00	2.47	2.25	0.63	2.00	1.00	1.28	10.34	0.78
Phyllariopsis brevipes	14.79	1.94	0.31	0.00	0.00	0.00	1.19	0.38	0.13	0.00	0.06	0.00	0.00	0.00	0.00	0.00	0.00	0.00	0.00	0.00	0.00
Phyllophora crispa	10.08	0.00	0.00	0.00	0.00	0.00	0.00	0.00	0.00	0.00	0.00	0.00	0.00	0.00	0.13	0.00	0.00	0.00	0.00	0.00	0.00
Plocamium cartilagineum	12.84	3.00	0.44	0.06	0.06	0.31	0.50	9.41	16.56	8.88	3.47	31.88	20.94	0.03	0.19	0.50	0.63	0.31	0.00	0.03	0.03
Plocamium fenestratum	15.60	0.00	0.00	0.00	0.00	0.00	0.00	0.00	0.00	0.00	0.00	0.00	0.00	0.00	0.00	0.00	0.00	0.00	0.59	0.00	0.00
Plocamium raphelisianum	8.81	0.00	0.00	0.00	0.00	0.00	0.00	0.00	0.66	0.00	0.00	0.00	0.00	0.00	0.06	0.00	0.00	0.00	0.00	0.00	0.00
Polysiphonia atlantica	16.71	0.00	0.00	0.00	0.00	0.00	0.00	0.03	0.00	0.00	0.00	0.00	0.00	0.91	0.00	0.00	0.09	0.00	0.00	0.00	0.00
Polysiphonia breviarticulata	17.04	0.00	0.00	0.00	0.00	0.00	0.00	0.00	0.00	0.00	0.00	0.00	0.00	0.00	0.00	0.03	0.03	0.00	0.00	0.00	0.00
Polysiphonia furcellata	11.66	0.00	0.00	0.00	0.00	0.00	0.00	0.00	0.03	0.00	0.00	0.00	0.00	0.00	0.00	0.00	0.00	0.00	0.00	0.00	0.00
Polysiphonia sertularioides	16.86	0.00	0.00	0.00	0.00	0.00	0.00	0.00	0.00	0.00	0.00	0.00	0.00	0.00	0.00	0.00	0.00	0.00	0.00	0.41	0.00
Polysiphonia subulata	14.64	0.00	0.00	0.00	0.00	0.00	0.00	0.00	0.00	0.00	0.00	0.00	0.00	0.00	0.00	0.00	0.00	0.00	0.06	0.00	0.00
Protohalopteris radicans	10.87	0.00	0.00	0.00	0.00	0.00	0.03	0.00	0.00	0.00	0.00	0.00	0.00	0.00	0.00	0.00	0.00	0.00	0.00	0.00	0.00
Pseudochlorodesmis furcellata	18.26	0.00	0.00	0.00	0.00	0.00	0.00	0.00	0.00	0.00	0.00	0.00	0.00	0.00	0.00	0.00	0.00	0.19	0.00	0.03	0.00
Pterocladiella capillacea	16.34	0.00	0.00	0.00	5.88	0.00	2.09	0.00	0.00	0.00	0.13	0.00	0.00	0.00	0.00	0.00	0.00	0.00	0.00	0.00	0.00
Pterosiphonia complanata	11.97	16.44	14.06	5.69	0.75	12.81	1.47	3.50	1.63	0.75	4.56	1.25	1.03	0.16	5.06	4.78	0.88	0.00	0.06	0.00	0.00
Pterothamnion crispum	11.67	0.00	0.00	0.06	0.00	0.03	0.03	0.47	0.22	1.91	0.22	0.72	0.00	0.00	0.38	0.03	0.00	0.00	0.00	0.00	0.00
Pterothamnion plumula	9.91	0.00	0.00	0.00	0.00	0.00	0.00	0.00	0.00	0.00	0.00	0.00	0.84	0.00	0.00	0.00	0.00	0.03	0.00	0.00	0.00
Rhodophyllis divaricata	9.93	0.00	0.00	0.00	0.03	0.00	0.00	0.03	0.00	0.00	0.00	0.63	0.03	0.41	0.00	0.00	0.03	0.44	0.75	0.06	0.66
Rhodymenia ardissonei	13.75	0.00	0.00	0.00	0.00	0.00	0.00	0.00	0.00	0.00	0.00	0.00	0.00	0.00	0.00	0.00	0.00	1.47	0.63	0.00	0.22
Rhodymenia delicatula	13.12	0.00	0.00	0.00	0.06	0.00	0.00	0.00	0.00	0.00	0.00	0.00	0.00	0.00	0.00	0.00	0.00	0.00	0.00	0.00	0.00
Rhodymenia holmesii	11.37	0.00	0.03	0.00	0.00	0.00	0.00	0.00	0.00	0.00	0.00	0.00	0.00	0.00	0.00	0.00	0.00	0.00	0.06	0.00	0.00
Rhodymenia pseudopalmata	15.92	0.00	0.00	0.00	0.06	0.97	0.03	0.13	0.97	1.91	1.81	6.75	6.06	0.03	0.16	0.00	0.00	0.00	0.00	0.00	0.00
Saccorhiza polyschides	10.26	55.94	99.38	100.0	73.44	48.44	58.31	9.41	0.25	0.00	0.00	0.00	0.00	0.00	0.00	0.00	0.00	0.00	0.00	0.00	0.00
Sargassum vulgare	19.18	0.00	0.00	0.00	0.00	0.00	0.00	0.00	0.00	0.00	0.00	0.00	0.00	0.00	0.00	0.00	0.00	0.03	0.22	1.41	7.03
Schizymenia dubyi	16.62	0.00	0.06	0.00	0.00	0.00	0.03	0.34	0.00	0.00	0.00	0.00	2.28	0.00	0.16	0.00	0.16	0.00	0.00	0.00	0.16
Scinaia furcellata	13.69	0.00	0.00	0.00	0.34	0.00	0.03	0.00	0.00	0.00	0.00	0.00	0.00	0.00	0.00	0.06	0.31	0.00	0.06	0.00	0.00
Seirospora interrupta	10.99	0.00	0.00	0.00	0.00	0.00	0.00	0.03	0.00	0.00	0.00	0.00	0.00	0.03	0.00	0.00	0.00	0.00	0.00	0.00	0.00
Seirospora sphaerospora	15.52	0.00	0.00	0.00	0.00	0.00	0.00	0.00	0.00	0.00	0.00	0.00	0.00	0.00	0.00	0.00	0.00	0.00	0.00	0.03	0.00
Spermothamnion flabellatum	13.07	0.00	0.00	0.00	0.00	0.00	0.00	0.00	0.00	0.00	0.00	0.00	0.00	0.00	0.00	0.00	0.00	0.00	0.00	0.06	0.00
Sphacelaria cirrosa	10.77	0.00	0.00	0.00	0.31	0.00	0.00	0.00	0.00	0.00	0.00	0.00	0.00	0.00	0.00	0.00	0.00	0.97	0.94	0.50	0.75
Sphacelaria rigidula	15.36	0.00	0.00	0.00	0.03	0.00	0.00	0.00	0.00	0.00	0.00	0.00	0.00	0.00	0.00	0.00	0.00	0.00	0.00	0.00	0.00
Sphaerococcus coronopifolius	11.54	0.00	0.19	0.00	0.87	2.03	0.06	2.50	1.06	0.63	2.81	0.00	0.00	0.00	0.00	0.63	2.69	0.00	0.00	0.00	0.00
Sphondylothamnion multifidum	10.45	0.00	0.13	0.00	0.09	0.03	0.00	0.00	0.00	0.00	0.00	0.00	0.00	0.03	0.94	0.25	0.16	0.00	0.00	0.00	0.06
Spyridia filamentosa	17.40	0.00	0.00	0.00	0.00	0.00	0.00	0.00	0.00	0.00	0.00	0.00	0.00	0.00	0.00	0.00	0.00	0.00	0.00	0.15	0.00
Taonia atomaria	14.31	2.06	0.00	0.28	0.00	0.00	0.00	0.00	0.34	0.00	0.19	0.06	0.00	0.88	1.34	3.06	0.38	0.28	0.09	0.00	0.13
Tricleocarpa fragilis	19.27	0.00	0.00	0.00	0.00	0.00	0.00	0.00	0.00	0.00	0.00	0.00	0.00	0.00	0.00	0.00	0.00	0.00	0.00	0.00	0.06
Ulva clathrata	15.87	0.00	0.00	0.00	0.00	0.00	0.00	0.00	0.00	0.00	0.00	0.00	0.00	0.00	0.00	0.00	0.00	0.28	0.53	4.69	0.00
Ulva polyclada	16.47	0.00	0.00	0.00	0.00	0.00	0.00	0.00	0.00	0.00	0.00	0.00	0.00	0.00	0.00	0.00	0.00	0.00	0.03	0.00	0.00
Ulva rigida	16.46	2.06	0.16	0.88	7.22	5.31	0.72	2.81	0.13	0.06	0.25	0.00	0.00	0.94	2.09	0.03	0.16	0.00	0.00	0.00	0.00
Umbraulva dangeardii	12.34	0.00	0.00	0.00	0.03	0.00	0.00	0.00	0.00	0.00	0.00	0.00	0.00	0.00	0.00	0.00	0.00	0.00	0.00	0.00	0.00
Valonia utricularis	18.97	0.00	0.00	0.00	0.00	0.00	0.00	0.00	0.00	0.00	0.00	0.00	0.00	0.00	0.00	0.00	0.00	0.06	0.63	0.19	0.22
*Vertebrata fruticulosa***	14.50	0.00	0.09	0.00	0.03	3.50	0.75	5.44	0.06	0.03	0.00	0.00	0.00	0.00	0.00	0.09	1.34	0.34	0.00	0.00	
Vertebrata furcellata	11.66	0.00	0.00	0.00	0.00	0.00	0.00	0.00	0.00	0.00	0.00	0.00	0.00	0.00	0.00	0.00	0.00	0.06	0.00	0.00	0.00
Vertebrata reptabunda	16.78	0.00	0.00	0.00	0.00	0.00	0.00	0.31	0.00	0.00	0.00	0.00	0.00	0.00	0.00	0.06	0.00	0.00	0.00	0.00	0.00
Vertebrata thuyoides	11.92	0.00	0.00	0.00	0.03	0.00	0.00	0.00	0.00	0.00	0.00	0.00	0.00	0.00	0.00	0.00	0.00	0.00	0.00	0.00	0.00
Wrangelia penicillata	19.01	0.00	0.00	0.00	0.00	0.00	0.00	0.00	0.00	0.00	0.00	0.00	0.00	0.00	0.00	0.00	0.00	1.03	0.75	4.03	2.19

(*continued on next page*)

(*continued*)

	TO	2015	2019	2015	2019	2015	2019	2015	2019	2015	2019	2015	2019	2015	2019	2015	2019	2015	2020	2015	2020
Xiphosiphonia ardreana	11.86	0.00	0.00	0.00	0.03	0.63	0.31	1.44	0.31	0.16	0.81	0.00	0.00	0.00	0.66	0.41	0.22	0.00	0.00	0.00	0.00
Xiphosiphonia pennata	14.40	0.00	0.00	0.00	0.00	0.00	0.16	0.09	0.53	0.00	0.19	0.00	0.00	0.00	0.00	0.00	0.31	0.00	0.06	0.00	0.00
Zanardinia typus	11.66	2.50	0.63	3.44	0.00	5.31	1.56	12.81	2.88	8.81	10.50	0.00	1.88	3.75	12.25	16.56	5.00	5.66	3.38	2.03	2.56

*Appendix f. Summary of PERMANOVA results testing for the effect of Location, Year, and the interaction of the two factors on the number of taxa. Pairwise comparisons for the factor Year for each location are shown at the bottom of the table. * The superscripts refer to the aggrupation of locations (no statistically significant differences)*

PERMANOVA- *permutational multivariate analysis of variance*

Source	Df	SS	MS	Pseudo-F	P (perm)	Unique perms
Year	1	487.58	487.58	1.4912	0.2465	9830
Location	9	13472	1496.9	50.661	0.0001	9952
Year X Location	9	2942.7	326.97	11.066	0.0001	9949
Res	300	8864.2	29.547			
Total	319	25767				

Pairwise comparison for the factor Year

Locations	t	p (perm)	Unique perms
L1	4.173	0.0005	40
L2	3.7514	0.0004	54
L3	2.4941	0.0203	67
L4	3.416	0.0027	75
L5	4.0842	0.0003	64
L6	6.8685	0.0001	21
L7	2.4041	0.0232	78
L8	0.38907	0.7189	71
L9	8.3172	0.0001	69
L10	2.3843	0.0286	46

*Pairwise comparison for the factor Location

2015: $L1^{a} = L2^{a} = L5^{a} = L7^{ab} = L4^{bc} = L3^{c} = L8^{c} = L9^{c} = L10^{c} \neq L6^{d}$

2019: $L1^{a} \neq L2^{b} = L5^{bc} = L7^{bcd} = L8^{bcd} = L3^{cd} = L10^{d} \neq L4^{e} \neq L6^{f} \neq L9^{g}$

Appendix g. Summary of DistLM analysis results and dbRDA coordinates scores for the relationship between temperature-related variables and multivariate communities (based on square-root transformed abundances and Bray-Curtis simmilarities). (*): variables selected in step-wise procedure based on AICc criterion and Best procedure

DistLM- *Distance based Linear Model*

MARGINAL TESTS

Variable	SS (Trace)	Pseudo-F	P	Proportion
SST (*)	12032	6.6967	0.0001	0.27116
Spring SST	11820	6.5362	0.0001	0.26639
Summer SST (*)	11152	6.0429	0.0001	0.25134

BEST SOLUTIONS

AICc	R^2	RSS	No.Vars	Selections
152.47	0.27116	32340	1	1
150.58	0.42341	25584	2	1;3
152.79	0.45033	24390	3	All

dbRDA COORDINATES SCORRES

Sample	dbRDA1	dbRDA2
15-L1	20,944	28,866
15-L2	25,234	16,252
15-L3	14,303	3,5562
15-L4	8,5111	−3,5409
15-L5	4,2282	−4,4984
15-L6	3,7388	−6,9842
15-L7	3,9521	−11,259
15-L8	−1,5566	−12,962
15-L9	−45,058	35,585
15-L10	−59,511	0,78942
19-L1	20,915	30,894
19-L2	22,286	21,67
19-L3	15,506	9,7165
19-L4	12,257	−12,188
19-L5	10,513	−20,397
19-L6	10,422	−18,095

(*continued on next page*)

(*continued*)

DistLM- *Distance based Linear Model*		
19-L7	9,5875	−23,083
19-L8	6,3314	−27,644
19-L9	−30,936	0,40116
19-L10	−51,668	−7,0802

*Appendix h. Summary of PERMANOVA results testing for the effect of Location, Year, and the interaction of the two factors on the Community Temperature Index. Pairwise comparisons for the factor Year for each location are shown at the bottom of the table. * the superscripts refer to the aggrupation of locations (no statistical significant differences)*

PERMANOVA- *permutational multivariate analysis of variance*						
Source	Df	SS	MS	Pseudo-F	P (perm)	Unique perms
Year	1	7.0246	7.0246	1.9673	0.1981	9827
Location	9	368.84	40.983	152.68	0.0001	9926
Year X Location	8	32.135	3.5706	13.302	0.0001	9940
Res	300	80.527	0.26842			
Total	319	488.53				
Pairwise comparison for the factor Year						
Locations	t	p (perm)	Unique perms			
L1	1.8112	0.0792	9842			
L2	2.0075	0.0535	9829			
L3	0.38874	0.7038	9838			
L4	3.2254	0.002	9849			
L5	3.6223	0.0011	9844			
L6	10.014	0.0001	9811			
L7	1.114	0.2744	9831			
L8	3.915	0.0009	9834			
L9	6.8481	0.0001	9836			
L10	4.2223	0.0002	9841			
Pairwise comparison for the factor Year						
2015: $L1^{ab} = L3^{a} = L6^{a} \neq L4^{b} = L5^{b} \neq L7^{c} = L8^{c} = L9^{c} \neq L2^{d} \neq L10^{e}$						
2019: $L1^{a} = L3^{a} \neq L4^{bd} = L5^{b} \neq L6^{c} = L8^{cd} \neq L2^{e} \neq L7^{f} \neq 9^{g} \neq L10^{h}$						

References

Accoroni, S., Percopo, I., Cerino, F., Romagnoli, T., Pichierri, S., Perrone, C., Totti, C., 2015. Allelopathic interactions between the HAB dinoflagellate *Ostreopsis* cf. *ovata* and macroalgae. Harmful Algae 49, 147–155. https://doi.org/10.1016/j.hal.2015.08.007.

Al-Ghussain, L., 2019. Global warming: Review on driving forces and mitigation. Environ. Prog. Sustain. Energy 38, 13–21. https://doi.org/10.1002/ep.13041.

Anadón, R., Fernández, C., García Flórez, L., Losada, I., Valdés, L., 2009. Evidencias y efectos potenciales del cambio climático en Asturias. 5. Costas y Océanos. In: Evidencias y efectos potenciales del cambio climático en Asturias, pp. 126–170. Consejería de Medio Ambiente, Ordenación del Territorio e Infraestructuras, Gobierno del Principado de Asturias. http://ria.asturias.es/RIA/bitstream/123456789/365/1/LIBRO%20COMPLETO_baja.pdf.

Anderson, B.C., 2006. Response of Tropical Marine Macroalgae to Thermal Stress. MSc. thesis. Florida Atlantic University, Boca Raton, FL.

Anderson, M.J., Gorley, R.N., Clarke, K.R., 2008. PERMANOVA+ for PRIMER: Guide to Software and Statistical Methods. PRIMER-E", Plymouth, UK.

Assis, J., Berecibar, E., Claro, B., Alberto, F., Reed, D., Raimondi, P., Serrão, E.A., 2017. Major shifts at the range edge of marine forests: the combined effects of climate changes and limited dispersal. Sci. Rep. 7, 44348 https://doi.org/10.1038/srep44348.

Baña, Z., Abad, N., Uranga, A., Azúa, I., Artolozaga, I., Unanue, M., Iriberri, J., Arrieta, J. M., Ayo, B., 2020. Recurrent seasonal changes in bacterial growth efficiency, metabolism and community composition in coastal waters. Environ. Microbiol. 22, 369–380. https://doi.org/10.1111/1462-2920.14853.

Benedetti-Cecchi, L., Pannacciulli, F., Bulleri, F., Moschella, P., Airoldi, L., Relini, G., Cinelli, F., 2001. Predicting the consequences of anthropogenic disturbance: large-scale effects of loss of canopy algae on rocky shores. Mar. Ecol. Prog. Ser. 214, 137–150. https://doi.org/10.3354/meps214137.

Borja, A., Chust, G., Fontán, A., Garmendia, J.M., Uyarra, M.C., 2018. Long-term decline of the canopy-forming algae *Gelidium corneum*, associated to extreme wave events and reduced sunlight hours, in the southeastern Bay of Biscay. Estuarine. Coastal Shelf Sci. 205, 152–160. https://doi.org/10.1016/j.ecss.2018.03.016.

Borja, Á., Egaña, J., Valencia, V., Franco, J., Castro, R., 2000. Estudio y validación de una serie de datos diarios de temperatura del agua del mar en San Sebastián, procedente de su Aquarium, 1947-1997 Ozeanografika 3, 139–152.

Borja, Á., Fontán, A., Muxika, I., 2013. Interactions between climatic variables and human pressures upon a macroalgae population: implications for management. Ocean Coast Manag. 76, 85–95.

Bowler, D., Böhning-Gaese, K., 2017. Improving the community-temperature index as a climate change indicator. PLoS One 12, e0184275. https://doi.org/10.1371/journal.pone.0184275.

Burrows, M.T., Bates, A.E., Costello, M.J., Edwards, M., Edgar, G.J., Fox, C.J., Halpern, B. S., Hiddink, J.G., Pinsky, M.L., Batt, R.D., García Molinos, J., Payne, B.L., Schoeman, D.S., Stuart-Smith, R.D., Poloczanska, E.S., 2019. Ocean community warming responses explained by thermal affinities and temperature gradients. Nat. Clim. Change 9, 959–963. https://doi.org/10.1038/s41558-019-0631-5.

Casado-Amezúa, P., Araújo, R., Bárbara, I., Bermejo, R., Borja, Á., Díez, I., Fernández, C., Gorostiaga, J.M., Guinda, X., Hernández, I., Juanes, J.A., Peña, V., Peteiro, C., Puente, A., Quintana, I., Tuya, F., Viejo, R.M., Altamirano, M., Gallardo, T., Martínez, B., 2019. Distributional shifts of canopy-forming seaweeds from the Atlantic coast of Southern Europe. Biodivers. Conserv. 28, 1151–1172. https://doi.org/10.1007/s10531-019-01716-9.

Chamberlain, S., Barve, V., Mcglinn, D., Oldoni, D., Desmet, P., Geffert, L., Ram, K., 2021. Rgbif: interface to the global biodiversity information facility API. https://CRAN.R-project.org/package=rgbif.

Chen, I.C., Hill, J.K., Ohlemüller, R., Roy, D.B., Thomas, C.D., 2011. Rapid range shifts of species associated with high levels of climate warming. Science 333, 1024–2015. https://doi.org/10.1126/science.1206432.

Cheng, L., Abraham, J., Trenberth, K.E., Fasullo, J., Boyer, T., Locarnini, R., Zhang, B., Yu, F., Wan, L., Chen, X., Song, X., Liu, Y., Mann, M.E., Reseghetti, F., Simoncelli, S., Gouretski, V., Chen, G., Mishonov, A., Reagan, J., Zhu, J., 2021. Upper ocean temperatures hit record high in 2020. Adv. Atmos. Sci. 38, 523–530. https://doi.org/10.1007/s00376-021-0447-x.

Chust, G., González, M., Fontán, A., Revilla, M., Alvarez, P., Santos, M., Cotano, U., Chifflet, M., Borja, A., Muxika, I., Sagarminaga, Y., Caballero, A., de Santiago, I., Epelde, I., Liria, P., Ibaibarriaga, L., Garnier, R., Franco, J., Villarino, E., Irigoien, X., Fernandes-Salvador, J.A., Uriarte, Andrés, Esteban, X., Orue-Echevarria, D., Figueira, T., Uriarte, A., 2022. Climate regime shifts and biodiversity redistribution in the Bay of Biscay. Sci. Total Environ. 803, 149622 https://doi.org/10.1016/j.scitotenv.2021.149622.

Clarke, K.R., Warwick, R.M., 2001. Change in Marine Communities, second ed. PRIMER-E Ltd, Plymouth.

Costoya, X., deCastro, M., Gómez-Gesteira, M., Santos, F., 2015. Changes in sea surface temperature seasonality in the Bay of Biscay over the last decades (1982–2014). J. Mar. Syst. 150, 91–101. https://doi.org/10.1016/j.jmarsys.2015.06.002.
Day, P.B., Stuart-Smith, R.D., Edgar, G.J., Bates, A.E., 2018. Species' thermal ranges predict changes in reef fish community structure during 8 years of extreme temperature variation. Divers. Distrib. 24, 1036–1046. https://doi.org/10.1111/ddi.12753.
deCastro, M., Gómez-Gesteira, M., Alvarez, I., Gesteira, J.L.G., 2009. Present warming within the context of cooling–warming cycles observed since 1854 in the Bay of Biscay. Continent. Shelf Res. 29 (8), 1053–1059. https://doi.org/10.1016/j.csr.2008.11.016.
Devictor, V., Julliard, R., Couvet, D., Jiguet, F., 2008. Birds are tracking climate warming, but not fast enough. Proceedings of the Royal Society B 275, 2743–2748. https://doi.org/10.1098/rspb.2008.0878.
Devictor, V., van Swaay, C., Brereton, T., Brotons, L., Chamberlain, D., Heliölä, J., Herrando, S., Julliard, R., Kuussaari, M., Lindström, Å., Reif, J., Roy, D.B., Schweiger, O., Settele, J., Stefanescu, C., Van Strien, A., Van Turnhout, C., Vermouzek, Z., WallisDeVries, M., Wynhoff, I., Jiguet, F., 2012. Differences in the climatic debts of birds and butterflies at a continental scale. Nat. Clim. Change 2, 121–124. https://doi.org/10.1038/nclimate1347.
Díez, I., Muguerza, N., Santolaria, A., Ganzedo, U., Gorostiaga, J.M., 2012. Seaweed assemblage changes in the eastern Cantabrian Sea and their potential relationship to climate change. Estuar. Coast Shelf Sci. 99, 108–120. https://doi.org/10.1016/j.ecss.2011.12.027.
Drouet, K., Jauzein, C., Herviot-Heath, D., Hariri, S., Laza-Martinez, A., Lecadet, C., Plus, M., Seoane, S., Sourisseau, M., Lemée, R., Siano, R., 2021. Current distribution and potential expansion of the harmful benthic dinoflagellate *Ostreopsis* cf. *siamensis* towards the warming waters of the Bay of Biscay, North-East Atlantic. Environ. Microbiol. 23 (9), 4956–4979. https://doi.org/10.1111/1462-2920.15406.
Falkenberg, L.J., Russell, B.D., Connell, S.D., 2013. Contrasting resource limitations of marine primary producers: implications for competitive interactions under enriched CO2 and nutrient regimes. Oecologia 172, 575–583. https://doi.org/10.1007/s00442-012-2507-5.
Fernández, C., 2016. Current status and multidecadal biogeographical changes in rocky intertidal algal assemblages: the northern Spanish coast. Estuarine. Coastal Shelf Sci. 171, 35–40. https://doi.org/10.1016/j.ecss.2016.01.026.
Fernández, C., 2011. The retreat of large brown seaweeds on the north coast of Spain: the case of *Saccorhiza polyschides*. Eur. J. Phycol. 46, 352–360. https://doi.org/10.1080/09670262.2011.617840.
Fernández-Salas, L.M., Durán, R., Mendes, I., Galparsoro, I., Lobo, F.J., Bárcenas, P., Rosa, F., Ribó, M., García-Gil, S., Ferrín, A., Carrara, G., Roque, C., Canals, M., 2015. Shelves of the iberian Peninsula and the balearic islands (I): morphology and sediment types. Bol. Geol. Min. 126, 327–376.
Filbee-Dexter, K., Wernberg, T., 2018. Rise of turfs: a new battlefront for globally declining kelp forests. Bioscience 68 (2), 64–76. https://doi.org/10.1093/biosci/bix147.
Flanagan, P.H., Jensen, O.P., Morley, J.W., Pinsky, M.L., 2019. Response of marine communities to local temperature changes. Ecography 42, 214–224. https://doi.org/10.1111/ecog.03961.
García, A.G., Olabarria, C., Alvarez-Losadaa, O., Viejo, R.M., 2021. Differential responses of trailing-edge populations of a foundation alga to thermal stres. Eur. J. Phycol. 56 (4), 373–388. https://doi.org/10.1080/09670262.2020.1842909.
GBIF.org, 2022. GBIF home page. https://www.gbif.org.
Gómez-Gesteira, M., deCastro, M., Alvarez, I., Gómez-Gesteira, J.L., 2008. Coastal sea surface temperature warming trend along the continental part of the Atlantic Arc (1985–2005). J. Geophys. Res. 113, C04010 https://doi.org/10.1029/2007JC004315.
Gómez-Gesteira, M., Gimeno, L., deCastro, M., Lorenzo, M., Alvarez, I., Nieto, R., Taboada, J., Crespo, A., Ramos, A., Iglesias, I., Gómez-Gesteira, J., Santo, F., Barriopedro, D., Trigo, I., 2011. The state of climate in NW Iberia. Clim. Res. 48, 109–144. https://doi.org/10.3354/cr00967.
González-Gil, R., González Taboada, F., Cáceres, C., Largier, J.L., Anadón, R., 2018. Winter-mixing preconditioning of the spring phytoplankton bloom in the Bay of Biscay. Limnol. Oceanogr. 63, 1264–1282. https://doi.org/10.1002/lno.10769.
Gorostiaga, J.M., 1995. Sublittoral seaweed vegetation of a very exposed shore on the Basque Coast (N. Spain). Bot. Mar. 38 https://doi.org/10.1515/botm.1995.38.1-6.9.
Gottfried, M., Pauli, H., Futschik, A., Akhalkatsi, M., Barančok, P., Benito Alonso, J.L., Coldea, G., Dick, J., Erschbamer, B., Fernández Calzado, M.R., Kazakis, G., Krajči, J., Larsson, P., Mallaun, M., Michelsen, O., Moiseev, D., Moiseev, P., Molau, U., Merzouki, A., Nagy, L., Nakhutsrishvili, G., Pedersen, B., Pelino, G., Puscas, M., Rossi, G., Stanisci, A., Theurillat, J.-P., Tomaselli, M., Villar, L., Vittoz, P., Vogiatzakis, I., Grabherr, G., 2012. Continent-wide response of mountain vegetation to climate change. Nat. Clim. Change 2, 111–115. https://doi.org/10.1038/nclimate1329.
Graba-Landry, A.C., Loffler, Z., McClure, E.C., Pratchett, M.S., Hoey, A.S., 2020. Impaired growth and survival of tropical macroalgae (*Sargassum* spp.) at elevated temperatures. Coral Reefs 39, 475–486. https://doi.org/10.1007/s00338-020-01909-7.
Guiry, M.D., Guiry, G.M., 2023. AlgaeBase. Worldwide Electronic Publication. National University of Ireland, Galway. https://www.algaebase.org. searched on 12 January 2023.
Harley, C.D.G., Anderson, K.M., Demes, K.W., Jorve, J.P., Kordas, R.L., Coyle, T.A., Graham, M.H., 2012. Effects of climate change on global seaweed communities. J. Phycol. 48, 1064–1078. https://doi.org/10.1111/j.1529-8817.2012.01224.x.
Husa, V., Sjøtun, K., Brattenborg, N., Lein, T.E., 2008. Changes of macroalgal diversity in sublittoral sites in southwest Norway: impact of an introduced species or higher temperature? Mar. Biol. Res. 4, 414–428. https://doi.org/10.1080/17451000802232874.
IPCC, 2023. AR6 Synthesis Report: Climate Change 2023. Synthesis Report of the IPCC Sixth Assessment Report (AR6): Summary for Policymakers.
Izquierdo, P., Rico, J.M., Taboada, F.G., González-Gil, R., Arrontes, J., 2022. Characterization of marine heatwaves in the Cantabrian Sea, SW bay of Biscay. Estuarine. Coastal Shelf Sci. 274, 107923 https://doi.org/10.1016/j.ecss.2022.107923.
Jian-Zhang, S., Xiu-Ren, N., Feng-Feng, L., Wan-Dong, C., Ding-Gen, Z., 2010. Long term changes of biodiversity of benthic macroalgae in the intertidal zone of the Nanji Islands. Acta Ecol. Sin. 30, 106–112. https://doi.org/10.1016/j.chnaes.2010.03.010.
Kortsch, S., Primicerio, R., Fossheim, M., Dolgov, A.V., Aschan, M., 2015. Climate change alters the structure of arctic marine food webs due to poleward shifts of boreal generalists. Proceedings of the Royal Society B 282, 20151546. https://doi.org/10.1098/rspb.2015.1546.
Kumagai, N.H., García Molinos, J., Yamano, H., Takao, S., Fujii, M., Yamanaka, Y., 2018. Ocean currents and herbivory drive macroalgae-to-coral community shift under climate warming. Proc. Nat. Acad. Sci. U.S.A. 115, 8990–8995. https://doi.org/10.1073/pnas.1716826115.
Lavín, A., Valdés, L., Sánchez, F., Abaunza, P., Forest, A., Boucher, J., Lazure, P., Anne Jegou, A.M., 2006. The Bay of Biscay: the encountering of the ocean and the shelf. In: Robinson, A.R., Brink, K.H. (Eds.), The Global Coastal Ocean: Interdisciplinary Regional Studies and Syntheses. Harvard Press, pp. 933–999.
Lazzari, P., Solidoro, C., Salon, S., Bolzon, G., 2016. Spatial variability of phosphate and nitrate in the Mediterranean Sea: a modeling approach. Deep-Sea Res. Part I Oceanogr. Res. Pap. 108, 39–52. https://doi.org/10.1016/j.dsr.2015.12.006.
Lemos, R.T., Pires, H.O., 2004. The upwelling regime off the West Portuguese Coast, 1941–2000. Int. J. Climatol. 24, 511–524. https://doi.org/10.1002/joc.1009.
Lindsey, R., Dahlman, L., 2022. National center for atmospheric research. Clim. Change: Global Temperature.
Lourenço, C.R., Zardi, G.I., McQuaid, C.D., Serrão, E.A., Pearson, G.A., Jacinto, R., Nicastro, K.R., 2016. Upwelling areas as climate change refugia for the distribution and genetic diversity of a marine macroalga. J. Biogeogr. 43, 1595–1607. https://doi.org/10.1111/jbi.12744.
McLean, M., Mouillot, D., Maureaud, A.A., Hattab, T., MacNeil, M.A., Goberville, E., Lindegren, M., Engelhard, G., Pinsky, M., Auber, A., 2021. Disentangling tropicalization and deborealization in marine ecosystems under climate change. Curr. Biol. 31, 4817–4823.e4815. https://doi.org/10.1016/j.cub.2021.08.034.
Merchant, C.J., Embury, O., Bulgin, C.E., Block, T., Corlett, G.K., Fiedler, E., Good, S.A., Mittaz, J., Rayner, N.A., Berry, D., Eastwood, S., Taylor, M., Tsushima, Y., Waterfall, A., Wilson, R., Donlon, C., 2019. Satellite-based time-series of sea-surface temperature since 1981 for climate applications. Sci. Data 6, 223. https://doi.org/10.1038/s41597-019-0236-x.
Monteiro, C., Pereira, J., Seabra, R., Lima, F.P., 2022. Fine-scale survey of intertidal macroalgae reveals recent changes in a cold-water biogeographic stronghold. Front. Mar. Sci. 9, 880074 https://doi.org/10.3389/fmars.2022.880074.
Muguerza, N., Arriaga, O., Díez, I., Becerro, M.A., Quintano, E., Gorostiaga, J.M., 2022a. A spatially-modelled snapshot of future marine macroalgal assemblages in southern Europe: towards a broader Mediterranean region? Mar. Environ. Res. 176, 105592 https://doi.org/10.1016/j.marenvres.2022.105592.
Muguerza, N., Díez, I., Quintano, E., Bustamante, M., Gorostiaga, J.M., 2017. Structural impoverishment of the subtidal vegetation of southeastern Bay of Biscay from 1991 to 2013 in the context of climate change. J. Sea Res. 130, 166–179. https://doi.org/10.1016/j.seares.2017.06.006.
Muguerza, N., Díez, I., Quintano, E., Gorostiaga, J.M., 2022b. Decades of biomass loss in the shallow rocky subtidal vegetation of the southeastern Bay of Biscay. Mar. Biodivers. 52, 28. https://doi.org/10.1007/s12526-022-01268-2.
Müller, R., Laepple, T., Bartsch, I., Wiencke, C., 2009. Impact of oceanic warming on the distribution of seaweeds in polar and cold-temperate waters. Bot. Mar. 52, 617–638. https://doi.org/10.1515/BOT.2009.080.
Muñiz, O., Rodríguez, J.G., Revilla, M., Laza-Martínez, A., Seoane, S., Franco, J., 2018. Seasonal variations of phytoplankton community in relation to environmental factors in an oligotrophic area of the European Atlantic coast (southeastern Bay of Biscay). Regional Studies in Marine Science 17, 59–72. https://doi.org/10.1016/j.rsma.2017.11.011.
NOAA National Centers for Environmental Information, 2022. Monthly Global Climate Report for Annual published online January 2023. https://www.ncei.noaa.gov/access/monitoring/monthly-report/global/202213. (Accessed 11 April 2023).
OBIS, 2022. Ocean Biodiversity Information System. Intergovernmental Oceanographic Commission of UNESCO. www.obis.org.
Orfanidis, S., 1991. Temperature responses and distribution of macroalgae belonging to the warm-temperate Mediterranean-Atlantic distribution group. Bot. Mar. 34, 12. https://doi.org/10.1515/botm.1991.34.6.541.
Orlando-Bonaca, M., Pitacco, V., Lipej, L., 2021. Loss of canopy-forming algal richness and coverage in the northern Adriatic Sea. Ecol. Indicat. 125, 107501 https://doi.org/10.1016/j.ecolind.2021.107501.
Ospina-Alvarez, N., Prego, R., Álvarez, I., deCastro, M., Álvarez-Ossorio, M.T., Pazos, Y., Campos, M.J., Bernárdez, P., Garcia-Soto, C., Gómez-Gesteira, M., Varela, M., 2010. Oceanographical patterns during a summer upwelling-downwelling event in the northern Galician rias: comparison with the whole ria system (NW of Iberian Peninsula). Continent. Shelf Res. 30, 1362–1372. https://doi.org/10.1016/j.csr.2010.04.018.
Parmesan, C., Yohe, G., 2003. A globally coherent fingerprint of climate change impacts across natural systems. Nature 421, 37–42. https://doi.org/10.1038/nature01286.
Pérez, F.F., Padín, X.A., Pazos, Y., Gilcoto, M., Cabanas, M., Pardo, P.C., Doval, M.D., Farina-Busto, L., 2010. Plankton response to weakening of the Iberian coastal

upwelling. Global Change Biol. 16, 1258–1267. https://doi.org/10.1111/j.1365-2486.2009.02125.x.
Perkol-Finkel, S., Airoldi, L., 2010. Loss and recovery potential of marine habitats: an experimental study of factors maintaining resilience in subtidal algal forests at the Adriatic Sea. PLoS One 5, e10791. https://doi.org/10.1371/journal.pone.0010791.
Pinsky, M.L., Selden, R.L., Kitchel, Z.J., 2020. Climate-driven shifts in marine species ranges: scaling from organisms to communities. Ann. Rev. Mar. Sci 12, 153–179. https://doi.org/10.1146/annurev-marine-010419-010916.
Poloczanska, E.S., Brown, C.J., Sydeman, W.J., Kiessling, W., Schoeman, D.S., Moore, P. J., Brander, K., Bruno, J.F., Buckley, L.B., Burrows, M.T., Duarte, C.M., Halpern, B.S., Holding, J., Kappel, C.V., O'Connor, M.I., Pandolfi, J.M., Parmesan, C., Schwing, F., Thompson, S.A., Richardson, A.J., 2013. Global imprint of climate change on marine life. Nat. Clim. Change 3, 919–925. https://doi.org/10.1038/nclimate1958.
Provoost, P., Bosch, S., 2019. "robis: R Client to Access Data from the OBIS API." Ocean Biogeographic Information System. Intergovernmental Oceanographic Commission of UNESCO. R package version 2.1.8. https://cran.r-project.org/package=robis.
R Development Core Team, 2023. R: A Language and Environment for Statistical Computing. R Foundation for Statistical Computing, Vienna, Austria. URL, Available at: https://www.R-project.org/.).
Ramos, E., Guinda, X., Puente, A., de la Hoz, C.F., Juanes, J.A., 2020. Changes in the distribution of intertidal macroalgae along a longitudinal gradient in the northern coast of Spain. Mar. Environ. Res. 157, 104930 https://doi.org/10.1016/j.marenvres.2020.104930.
Rhein, M., Rintoul, S.R., Aoki, S., Campos, E., Chambers, D., Feely, R.A., Gulev, S., Johnson, G.C., Josey, S.A., Kostianoy, A., Mauritzen, C., Roemmich, D., Talley, L.D., Wang, F., 2013. Observations: ocean. In: Stocker, T.F., Qin, D., Plattner, G.-K., Tignor, M., Allen, S.K., Boschung, J., Nauels, A., Xia, Y., Bex, V., Midgley, P.M. (Eds.), Climate Change 2013: the Physical Science Basis. Contribution of Working Group I to the Fifth Assessment Report of the Intergovernmental Panel on Climate Change. Cambridge University Press, Cambridge, United Kingdom and New York, NY, USA.
Rönnbäck, P., Kautsky, N., Pihl, L., Troell, M., Söderqvist, T., Wennhage, H., 2007. Ecosystem goods and services from Swedish coastal habitats: identification, valuation, and implications of ecosystem shifts. AMBIO A J. Hum. Environ. 36, 534–544. https://doi.org/10.1579/0044-7447(2007)36[534:EGASFS]2.0.CO;2.
RStudio Team, 2016. RStudio. Integrated development for R. RStudio, Inc., Boston, MA. http://www.rstudio.com/.
Serret, P., Fernández, E., Sostres, J.A., Anadón, R., 1999. Seasonal compensation of microbial production and respiration in a temperate sea. Mar. Ecol. Prog. Ser. 187, 43–57. https://doi.org/10.3354/MEPS187043.
Shaltout, M., Omstedt, A., 2014. Recent sea surface temperature trends and future scenarios for the Mediterranean Sea. Oceanologia 56, 411–443. https://doi.org/10.5697/oc.56-3.411.
Sjøtun, K., Husa, V., Asplin, L., Sandvik, A., 2015. Climatic and environmental factors influencing occurrence and distribution of macroalgae - a fjord gradient revisited. Mar. Ecol. Prog. Ser. 532, 73–88. https://doi.org/10.3354/meps11341.
Smale, D.A., Wernberg, T., 2013. Extreme climatic event drives range contraction of a habitat-forming species. Proceedings of the Royal Society B 280, 20122829. https://doi.org/10.1098/rspb.2012.2829.
Steller, D., Hernandez-Ayón, J., Riosmena-Rodríguez, R., Cabello-Pasini, A., 2007. Effect of temperature on photosynthesis, growth and calcification rates of the free-living coralline alga Lithophyllum margaritae. Cienc. Mar. 33, 441–456. https://doi.org/10.7773/cm.v33i4.1255.
Steneck, R.S., Graham, M.H., Bourque, B.J., Corbett, D., Erlandson, J.M., Estes, J.A., Tegner, M.J., 2002. Kelp forest ecosystems: biodiversity, stability, resilience and future. Environ. Conserv. 29, 436–459. https://doi.org/10.1017/S0376892902000322.
Stuart-Smith, R.D., Edgar, G.J., Barrett, N.S., Kininmonth, S.J., Bates, A.E., 2015. Thermal biases and vulnerability to warming in the world's marine fauna. Nature 528, 88–92. https://doi.org/10.1038/nature16144.
Tittensor, D.P., Mora, C., Jetz, W., Lotze, H.K., Ricard, D., Berghe, E.V., Worm, B., 2010. Global patterns and predictors of marine biodiversity across taxa. Nature 466, 1098–1101. https://doi.org/10.1038/nature09329.
Valdes-Abellan, J., Pardo, M.A., Tenza-Abril, A.J., 2017. Observed precipitation trend changes in the western Mediterranean region: observed precipitation trends in western Mediterranean. Int. J. Climatol. 37, 1285–1296. https://doi.org/10.1002/joc.4984.
Valencia, V., Franco, J., Borja, A., Fontán, A., 2004. Hydrography of the south-eastern bay of Biscay. In: Borja, A., Collins, M. (Eds.), Oceanography and Marine Environment of the Basque Country, vol. 70. Elsevier Oceanography Series, pp. 159–187. https://doi.org/10.1016/S0422-9894(04)80045-X.
Vergés, A., Steinberg, P.D., Hay, M.E., Poore, A.G.B., Campbell, A.H., Ballesteros, E., Heck, K.L., Booth, D.J., Coleman, M.A., Feary, D.A., Figueira, W., Langlois, T., Marzinelli, E.M., Mizerek, T., Mumby, P.J., Nakamura, Y., Roughan, M., van Sebille, E., Gupta, A.S., Smale, D.A., Tomas, F., Wernberg, T., Wilson, S.K., 2014. The tropicalization of temperate marine ecosystems: climate-mediated changes in herbivory and community phase shifts. Proceedings of the Royal Society B 281, 20140846. https://doi.org/10.1098/rspb.2014.0846.
Voerman, S.E., Llera, E., Rico, J.M., 2013. Climate driven changes in subtidal kelp forest communities in NW Spain. Mar. Environ. Res. 90, 119–127. https://doi.org/10.1016/j.marenvres.2013.06.006.
Webb, T.J., Lines, A., Howarth, L.M., 2020. Occupancy-derived thermal affinities reflect known physiological thermal limits of marine species. Ecol. Evol. 10, 7050–7061. https://doi.org/10.1002/ece3.6407.
Wernberg, T., Bennett, S., Babcock, R.C., de Bettignies, T., Cure, K., Depczynski, M., Dufois, F., Fromont, J., Fulton, C.J., Hovey, R.K., Harvey, E.S., Holmes, T.H., Kendrick, G.A., Radford, B., Santana-Garcon, J., Saunders, B.J., Smale, D.A., Thomsen, M.S., Tuckett, C.A., Tuya, F., Vanderklift, M.A., Wilson, S., 2016. Climate-driven regime shift of a temperate marine ecosystem. Science 353, 169–172. https://doi.org/10.1126/science.aad8745.